Diploma Thesis: Worldwide seismicity in view of Non Extensive Statistical Physics

Heraklio,2015

CHOCHLAKI KALLIOPI

(3485)

kalliopi@outlook.com

Supervisor: Dr Filippos Vallianatos

Department of Physics, University of Crete

Acknowledgments

First of all, I would like like to thank my supervisor professor, Filippos Vallianatos for all the help, the ideas and the time that he dedicated during the preparation of the thesis but mostly for his support and trust in me during this work. I am very grateful for all the things I learned from him and I hope to have the chance to collaborate again with him in the future.

I would also like to thank professor George Tsironis, who was willing to help and guide us despite his busy schedule. I feel very grateful for his contribution and the time he dedicated.

I also feel the need to give many thanks to George Michas, George Chatzopoulos and Emmanouel Karamalegos, who were always more than willing to help me with all the necessary programming knowledge.

Last, I wish to thank my friends and family for their love and support during this period.

Statement of the problem

Earthquakes have always been one the most intriguing natural phenomena for the mankind. However, the complexity of the earth's interior makes the investigation of this system more and more complicated. Among the years many models have been proposed for the description of the seismic behavior and the last years has been made significant progress, since now we are in position to understand many aspects of the seismic behavior and how this extremely complex system works. The most promising and adequate model for describing systems such as the Earth seems to be the Non Extensive Statistical Physics model, introduced by Tsallis in 1988. This model is strongly supported by the fact that this type of statistical mechanics is the appropriate methodological tool to describe entities with (multi) fractal distributions of their elements and where long-range interactions or intermittency are important, as in earthquakes. The NESP approach starting from the classic Boltzman-Gibbs statistics develops an entire model , based on the maximization of the Tsallis entropy, that gives us the opportunity to study the collective properties of even very large earthquakes (mega earthquakes), such as the earthquake occurred occurred in Sumatra (2004) with magnitude Mw=9.0 and the recent Japan mega earthquake with magnitude Mw=9.1 (2011) .

In the present work we study the distribution of worldwide shallow strong seismic events occurred from 1981 to 2011 extracted from the CMT catalog, with magnitude equal or greater than Mw5.0. Our analysis based on the subdivision of the Earth surface into seismic zones that are homogeneous with regards to seismic activity and orientation of the predominant stress field. We analyze the magnitude-frequency distribution along with the interevent time distribution between successive earthquakes using the Tsallis entropy approach in each of the seismic zones.

Our aim is to understand how this model works, under which conditions is valid and how non extensive parameters, such as the entropic index qM and qT , extracted from the frequency magnitude and interevent time distributions respectively, are affected by factors such as the magnitude threshold and the earthquake depth and finally what information can we extract by applying the NESP model in global seismicity catalogs.

The present thesis is organized as follow:

CHAPTER 1: Theoretical background

CHAPTER 2: Methodology and Results

CHAPTER 3: CONLUSIONS

CHAPTER 4: REFERENCES

CHAPTER 1: Theoretical background

1.1 The Gutenberg-Richter Law

Although it is very difficult to explore the behavior of complex dynamic systems, such as the Earth's interior, which is characterized by inhomogeneous areas with different seismic activity, some simple empirical relations are valid, such as the Gutenberg-Richter law (1944), which gives the relationship between the frequency and magnitude of earthquakes. The Gutenberg-Richter law (hereafter, GR law), is an empirical relation between the magnitude M of a seismic event and the number of events N(>M) with magnitude higher than M, introduced in 1944 by Beno Gutenberg and Charles Richter. The mathematical expression of the GR law is:

$$\log N(M)=a-bM \qquad (1.1)$$

,where a,b are constants for a fixed earthquake data set.

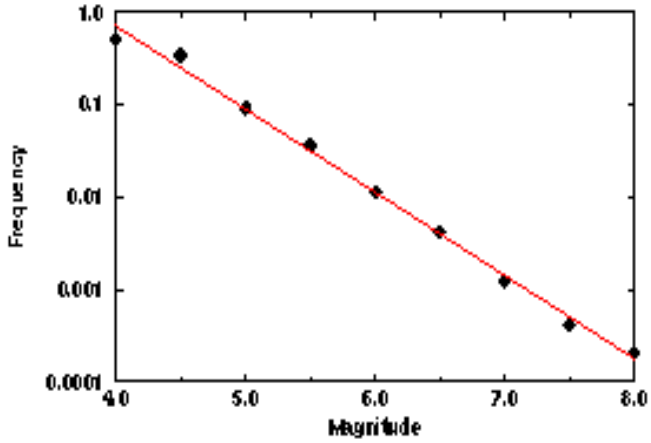

Figure 1.1.1: frequency-magnitude distribution according to the Gutenberg-Richter law (extracted from simscience.org)

By plotting on a logarithmic scale the number of earthquakes higher than or equal to the magnitude M, in a predefined period of time, against magnitude, we determine the b-value of the above equation, which is a basic characteristic of the seismicity rate and for most regions is close to unity (b≈1).

1.2 Boltzmann-Gibbs entropy

The term “entropy” was introduced in statistical mechanics, in order to to explain the behavior of macroscopic systems in terms of the dynamical laws governing their microscopic consituents. Boltzmann was the first to propose a probabilistic definition of entropy, characterizing it as “ a measure of disorder” of the system suggesting the following equation:

$$S = K \ln W \qquad (1.2)$$

Where K refers to the Boltzmann’s constant and *W* to the number of microstates corresponding to a given macrostate. The above form was refined a few years later by Gibbs leading to the now known Boltzmann-Gibbs entropy expressed by:

$$S_{BG} = -K_B \sum_i^W Pi \ln Pi \qquad (1.3)$$

where

$$\sum_i^W Pi = 1 \qquad (1.4)$$

for a set of W discrete states and

$$S_{BG} = -K_B \int dx P(x) ln[sP(x)] \qquad (1.5)$$

with

$$\int dx\, P(x) = 1 \qquad (1.6)$$

when the appropriate variable is a continuous one.

In this form, $x/s \in R^D$, $D \geq 1$ being the dimension of the full space of microscopic states where x and s carry the same physical units as x, so that x/s is a dimensionless.

In general, for at least two different values of i , $P_i < 1$ so the main form transforms to:

$$S_{BG} = -k_B \langle \ln P_i \rangle = k \langle \ln \frac{1}{Pi} \rangle \qquad (1.7)$$

As a conclusion, the B-G entropy is always positive, except if we know with certainty the state of the system, in which case we can easily conclude that $S_{BG}=0$. The B-G entropy also has its maximum at equal probabilities and it is expansable, which means that if we add at the system a new state with zero probability the entropy remains unaffected. In mathematicals terms this is translated as:

$$S_{BG}(P_1, P_2, \ldots, P_W, 0) = S_{BG}(P_1, P_2, \ldots, P_W) \qquad (1.8)$$

If two states A, B are independent then:

$$S_{BG}(A+B) = S_{BG}(A) + S_{BG}(B) \qquad (1.9)$$

Therefore, the B-G entropy is additive.

1.3 Non-extensive statistical physics

The concept of the classical Boltzmann- Gibbs statistical mechanics explains perfectly the behavior of classical systems, however in more complex systems, where long-range interactions are important, this model does not seem to be the most adequate tool for describing them. This leads to the conclusion that the B-G statistical mechanics has its limitations and at this point a new framework is introduced in 1988 by Constantino Tsallis, (Tsallis,1988) named non extensive statistical physics (Tsallis, 1998). Non-extensive statistical physics refers to the non-additive entropy S_q (Tsallis 2009), which is an advanced form of Boltzmann-Gibbs (BG) entropy, introducing an entropic expression symbolized as "q", which reflects the degree of non-additivity. The Tsallis entropy, S_q is defined as:

$$S_q=K_B\frac{1-\sum_{i=1}^{W} Pi^q}{q-1} \quad , q \in R \qquad (1.10)$$

Where K_B is Boltzmann's constant, W is the total number of microscopic configurations and P_i is a set of probabilities. When q=1, Boltzmann-Gibbs statistical mechanics is recovered ($S_1=S_{BG}$).
In contrast to the Boltzmann-Gibbs entropy, the Tsallis entropy is non-additive. Specifically, for two probabilistic independent events A, B:

$$\frac{Sq(A+B)}{k} = \frac{Sq(A)}{k} + \frac{Sq(B)}{k} + (1-q)\frac{Sq(A)}{k}\frac{Sq(B)}{k} \qquad (1.11)$$

Using the Lagrange multipliers method we can maximize the non-extensive entropy under appropriate conditions in order to find the probability distribution P(X) of a certain parameter X.

The Tsallis entropy can be also expressed in an integrated formulation as (Abe and Suzuki, 2005) :

$$S_q=k_B\frac{1-\int P^q(X)dX}{q-1} \qquad (1.12)$$

With the normalization condition:

$$\int_0^{\infty} P(X)dX = 1 \qquad (1.13)$$

where P_q stands for the escort probability:

$$P_q(X)=\frac{P^q(X)}{\int_0^{\infty} P^q(X)dX} \qquad (1.14)$$

The probability distribution after applying the Lagrange multipliers method is given as:

$$P(X)=\frac{[1-(1-q)Bq]^{1/1-q}}{Z_q} = \frac{\exp(-BqX)}{Z_q} \qquad (1.15)$$

Where the q-exponential function is defined as :

$$\exp_q(X)=\begin{cases}[1+(1-q)X]^{1/1-q} & \text{when } [1+(1-q)X] \geq\geq 0 \quad (1.16)\\ 0 & \text{,when } [1+(1-q)X]<0 \quad (1.17)\end{cases}$$

The inverse given by the expression of the q-exponential is the q-logarithmic function :

$$\ln(q)=\frac{1}{1-q}(X^{1-q}-1) \qquad (1.18)$$

1.4 The frequency-magnitude distribution according to NESP

It is already mentioned that the energy distribution of earthquakes exhibit power law decay, as it is previsedby the G-R law (Gutenberg and Richter, 1942). In 2004 a new model for earthquake's dynamics was proposed by Sotolongo and Posadas (Sotolongo and Posadas, 2004), based on a non-extensive formalism. They introduced a new relationship that describes the cumulative distribution of the number of events N greater than the magnitude M in a seismic region, in which the G-R law is considered as a particular case. Since fragments are the result of the violent fractioning between the fault planes then long-range interactions are expected between the existent fragments.

If P(s) express the probability of finding a fragment of surface s and $\int P^q(s)ds$: the sum of all possible states, then the Tsallis entropy S_q is given by:

$$S_q=k_B\frac{1-\int P^q(s)ds}{q-1} \qquad (1.19)$$

Where the probability P(s) is obtained under the constrain that it is normalized according to the equation:

$$\int_0^\infty P(s)ds=1 \qquad (1.20)$$

And the q expectation value obeys the condition:

$$s_q=\langle s\rangle_q=\frac{\int_0^\infty \sigma P^q(s)ds}{\int_0^\infty P^q(s)ds} \qquad (1.21)$$

By using the Lagrange-multipliers technique we obtain:

$$\delta S_q^*=\delta(S_q+\alpha\int_0^\infty p(s)ds-\beta s) \qquad (1.22)$$

where α,β represent the Lagrange multipliers.

After some algebra, we arrive at the following relationship for the fragment size distribution function:

$$P(s)=\left[1-\frac{(1-q)}{(2-q)}(s-s_q)\right]^{1/1-q} \quad (1.23)$$

The proportionality between the released energy E and the tree dimensional size of the fragments (r^3) now becomes:

$$s-s_q=(\frac{E}{a_E})^{2/3} \quad (1.24)$$

Introducing (1.24) to (1.23), the energy distribution function can be written (Telesca, 2012) as:

$$P(E)=\frac{1}{\frac{dE}{d\sigma}}P\left[(\frac{E}{a_E})^{2/3}+s_q\right]=\frac{ds}{dE}\left[1-\frac{(1-q)}{(2-q)}(\frac{E}{\alpha_E})^{2/3}\right]^{\frac{1}{1-q}} \quad (1.25)$$

where $\frac{ds}{dE}$ can be obtained by changing equation (1.24) into:

$$\frac{ds}{dE}=\frac{2}{3}\frac{E^{-1/3}}{{a_E}^{2/3}}dE \quad (1.26)$$

Using the aforementioned expression we lead to the probability distribution function P(E) as:

$$P(E)=\frac{C_1E^{-1/3}}{\left[1+C_2E^{2/3}\right]^{\frac{1}{q-1}}} \quad (1.27)$$

with $C_1=\frac{2}{3{a_E}^{2/3}}$ and $C_2=-\frac{(1-q)}{(2-q){a_E}^{2/3}}$

In the latter expression, the probability of the energy is $P(E)=n(E)/N_0$, where n(E) corresponds to the number of earthquakes with energy E and N_0 is the total number of earthquakes. A more viable expression can now be obtained by introducing the normalized cumulative number of earthquakes given by the integral of Eq. (1.25):

$$\frac{N(E>E_{th})}{N_0}=\int_{E_{th}}^{\infty}P(E)dE \quad (1.28)$$

where N(E > Eth) is the number of earthquakes with energy E greater than the threshold energy E_{th} and N_0 the total number of earthquakes. Introducing eq. (1.27) to (1.28) we lead to:

$$\frac{N(E>E_{th})}{N_0} = \left[1 - (\frac{1-q_E}{2-q_E})(\frac{E}{a_E})^{2/3}\right]^{\frac{2-q_E}{1-q_E}} \qquad (1.29)$$

Considering that $M \approx \frac{2}{3}\log(E)$ (Kanamori, 1978) we can easily derive :

$$\frac{N(>M)}{N} = \left[1 - (\frac{1-q_E}{2-q_E})(\frac{10^M}{{a_E}^{2/3}}\right]^{\frac{2-q_E}{1-q_E}} \qquad (1.30)$$

The constant a_E expresses the proportionality between the released energy E and the fragment size r, while q is the entropic index that from now on we will refer to as q_E. Applying the above model in various geotectonic environments, it seems to describe better the earthquake energy distribution in a wide range of magnitudes than the G-R law, which above some threshold magnitude can be considered as a particular case of the non-extensive model of eq. (1.30) with $b=(2-q_E)/(q_E-1)$.

1.5 Interevent times distribution

Applying the Boltzmann-Gibbs statistical mechanics in the probability distribution of a set of uncorrelated events, we expect as a result a Poisson distribution. But when we apply the known models of B-G mechanics in an earthquake catalog, we notice a deviation from the expected exponential distribution, which leads to the conclusion that long-range correlations do exist at the interevent times series. Several analysis of the temporal space between successive earthquakes have been done over the years and they have evidenced that the seismic time series undergoes over several transitions between quasi-equilibrium states, each of which obeys the aforementioned q exponential distribution with q greater than 1, which is derived after maximization of Tsallis entropy S_q (Abe and Suzuki, 2005). The q-exponential distribution consists a generalization of the Zipf-Mandelbrot distribution (Mandelbrot, 1983), where the standard Zipf-Mandelbrot distribution corresponds to the case q>1 (Abe and Suzuki, 2003). In the limit $q \rightarrow 1$ the q-exponential and q-logarithmic functions lead to the ordinary exponential and logarithmic functions respectively. If q>1 asymptotic power-law behavior is observed with slope -1/(q-1). In contrast, for 0<q<1 a cut-off appears (Abe and Suzuki 2003).

More detailed, if P(T) : the interevent times (T) distribution and if we assume $K_B \sim 1$ the entropy S_q becomes:

$$S_q = \frac{1-\int_0^{\infty} P^q(T)dT}{q-1} \qquad (1.31)$$

under the normalization: $\int_0^{\infty} P(T)dT = 1$ and the condition for the q- expectation value (Tsallis,2009): $T_q = < T >_q = \frac{\int_0^{\infty} P^q(T)dT}{\int_0^{\infty} P^q(T)dT}$

Applying the Lagrange multipliers method we lead to:

$$\delta S_q = \delta(S_q - a\int_0^{T_{max}} P(t)dT - \beta T_q) = 0 \qquad (1.32)$$

where α and β represent the Lagrange multipliers. Thus we obtain the physical probability:

$$P(T) = \frac{\left[1-(1-q)B_qT\right]^{1/(1-q)}}{Z_q} = \frac{\exp_q(-B_qT)}{Z_q} \qquad (1.33)$$

where Z_q is the q-partition function

$$Z_q = \int_0^{t_{max}} exp_q\left(-B_qT\right)dt \qquad (1.34)$$

with $B_q = \frac{\beta}{C_q-(1-q)\beta t_q}$ and $C_q = \int_0^{t_{max}} p^q(T)dT$ (1.35)

The inverse of the above equation is the q-logarithmic function already presented in chapter 1.2 (eq. (1.18))

1.6 Earth's seismicity and seismic zones

Since the seismic activity of the earth is not homogeneous there was a need to subdivide the Earth's surface in zones that are homogeneous and have similar seismic behavior. For the purpose of our analysis, we used the Flinn-Engdahl regionalization technique, also known as F-E code (Flinn, Engdahl and Hill, 1974), which was originally introduced in 1974 and revised in 1995(Young, 1995).

The F-E Region sceme is a list of boundary definitions used by Earth scientists in order to identify the geotectonic regions of the Earth. The original regionalization was achieved by Gutenberg-Richter (Gutenberg and Richter, 1954), who created a map with 51 regions from which the regions with high seismicity where smaller in area than those of low seismicity.

As a result, the oceanic regions, which are less seismically active, covered the biggest part of the map.

The F-E regionalization is a reorganization of the Gutenberg-Richter division and consists of 50 large areas called “seismic regions” and 729 subdivisions completing the puzzle, called “geographical regions”. In our study, we only used the seismic regions,presented in table 1.6.1.

Region 1	**Alaska - Aleutian Arc**
Region 2	**Southeastern Alaska to Washington**
Region 3	**Oregon, California and Nevada**
Region 4	**Baja California and Gulf of California**
Region 5	**Mexico - Guatemala Area**
Region 6	**Central America**
Region 7	**Caribbean Loop**
Region 8	**Andean South America**
Region 9	**Extreme South America**
Region 10	**Southern Antilles**
Region 11	**New Zealand Region**
Region 12	**Kermadec - Tonga - Samoa Basin Area**
Region 13	**Fiji Islands Area**
Region 14	**Vanuatu Islands**
Region 15	**Bismarck and Solomon Islands**
Region 16	**New Guinea**
Region 17	**Caroline Islands Area**
Region 18	**Guam to Japan**
Region 19	**Japan - Kuril Islands - Kamchatka Peninsula**
Region 20	**Southwestern Japan and Ryukyu Islands**
Region 21	**Taiwan Area**
Region 22	**Philippine Islands**
Region 23	**Bornea – Sulawesi**
Region 24	**Sunda Arc**
Region 25	**Myanmar and Southeast Asia**
Region 26	**India - Xizand - Sichuan - Yunnan**
Region 27	**Southern Xinjiang to Gansu**
Region 28	**Lake Issyk-Kul to Lake Baykal**
Region 29	**Western Asia**
Region 30	**Middle East - Crimea - Eastern Balkans**
Region 31	**Western Mediterranean Area**
Region 32	**Atlantic Ocean**
Region 33	**Indian Ocean**
Region 34	**Eastern North America**
Region 35	**Eastern South America**
Region 36	**Northwestern Europe**

Region 37	**Africa**
Region 38	**Australia**
Region 39	**Pacific Basin**
Region 40	**Arctic Zone**
Region 41	**Eastern Asia**
Region 42	**Northeasterb Asia, Northern Alaska to Greeland**
Region 43	**Southeastern & Antarctic Pacific Ocean**
Region 44	**Galapagos Islands Area**
Region 45	**Macquarie Loop**
Region 46	**Andaman Islands to Sumatera**
Region 47	**Baluchistan**
Region 48	**Hindu Kush and Pamir Area**
Region 49	**Northern Eurasia**
Region 50	**Antarctica**

Table 1.6.1 : The Flinn- Engdahl regions

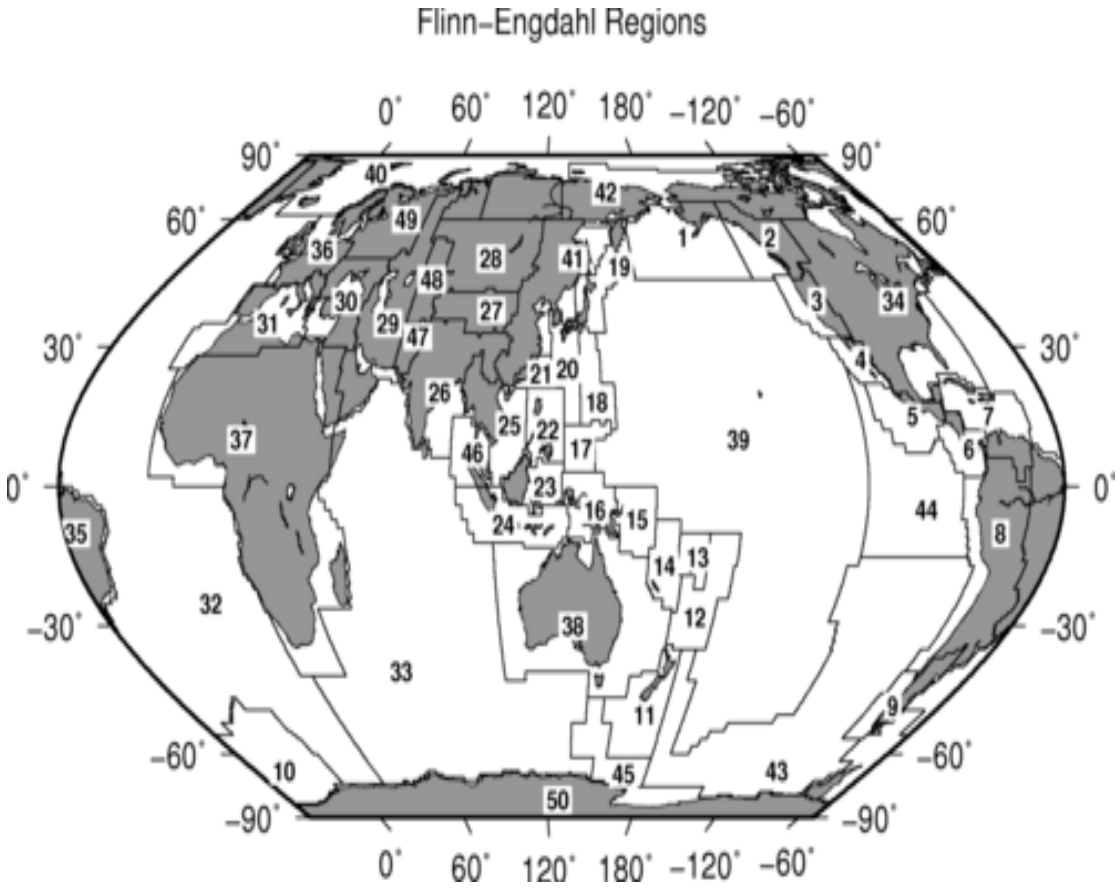

Figure 1.6.1: Map of the Flinn-Engdahl seismic Regions

Lombardi and Marzzochi (2007) merged some of the above seismic regions into larger tectonically homogeneous zones, applying a new regionalization technique. They computed a representative mean focal mechanism for each one of the 50 zones using the cumulative moment tensor method introduced by Kostrov (1974), which consists of summing all moment tensors of the earthquakes in a given area and then computing the best double couple for this cumulative tensor. As a result, the 50 regions decreased to 39, as shown in figure 1.6.2.

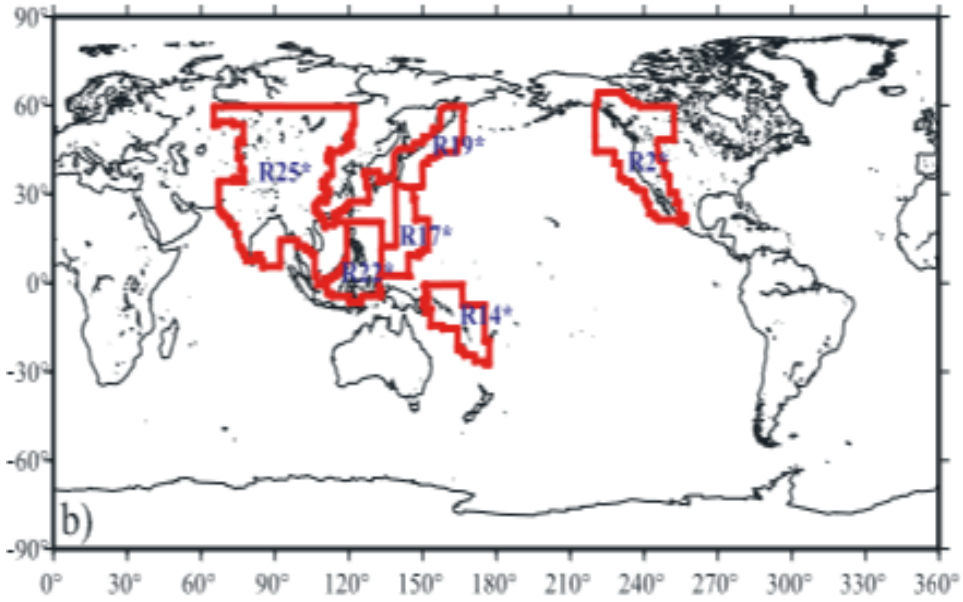

Figure 1.6.2: Lombardi and Marzocchi's regionalization

The new zones are now marked with asterisk and explained in table 1.5.2:

New Zones	FE regions
R2*	2-3-4
R14*	14-15
R17*	17-18
R19*	19-20-21
R22*	22-23
R25*	25-26-27-28-47

Table 1.6.2: The new zones created by Lombardi and Marzocchi

1.7 Declustering the earthquake catalog

Every independent earthquake that occurs leads to triggering new earthquakes known as aftershocks while all the events occurred during the preparatory stage are termed as foreshocks. Since there is no way to distinguish these dependent events from the independent one from just their waveform, there was a need to create an algorithm that could isolate the “mother earthquake”, which is caused by tectonic loading and natural processes from the earthquakes born due to the first one. This is exactly the purpose of “ declustering”, to remove the foreshocks and aftershocks, that form clusters and isolate a catalog that consists of only mainshocks. Over the years, many declustering methods have been proposed and used by seismologist and, among them, the Reasenberg method (Reasenberg, 1985) which we are going to use in our study.

Reasenberg’s method is based on identifying the dependent earthquakes according to spatial and temporal interaction zones. The process of more and more aftershocks has as a result the extension of the earthquake clusters. The spatial extent of the interaction zone is chosen according to stress distribution near the “mother earthquake” and leads to an after-slip as shown in figure 1.5.3.

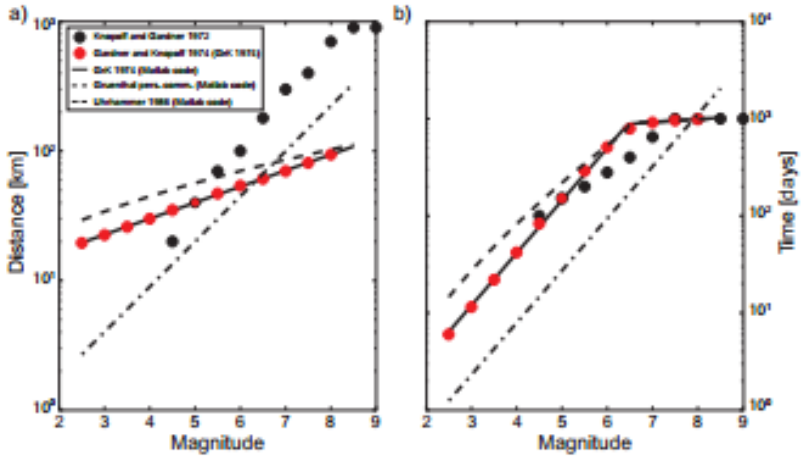

Figure 1.7.3: Aftershocks identification windows in space (a) and in time (b)

The spatial interaction relation is expressed by (Molchan and Dmitrieva, 1992) :

$$\log d(km) = 0,4M_0 - 1,943 + k \qquad (1.36)$$

where k=1 for the distance to the largest earthquake and 0 for the distance to the last one. The temporal extension is based on the Omori law (Omori, 1894), expressed by the following equation:

$$n(t) = \frac{k}{(c+t)^p} \qquad (1.37)$$

Where n(t) refers to the rate of events, p modifies the decay and typically falls in the range 0.7-1.5 and k, c are fitting coefficients.

All linked events define a cluster, in which the largest earthquake is considered as the mainshock and the rest of them as aftershocks and foreshocks. So, providing in our program an earthquake catalog which contains information about the space, time and magnitude of the events, we can easily take back the cluster and the new declustered catalog.

CHAPTER 2: Methodology and Results

To analyze the global seismicity a seismic catalog than contains all the seismic events with magnitude Mw greater than 5.0 from 1/01/1981 until 31/12/2011 and seismic depth until 50 kilometers was created. Our source was the global centroid moment tensor catalog hosted in www.globalcmt.org. We subdivided the whole catalog into subcatalogs each of which contains events from 5 successive years with a three-year overlap, so that we can obtain a smooth transition over time. Furthermore, we analyze the seismicity evolved in the zone defined by the Flinn-Engdahl regionalization.

2.1 Calculation of b-value of the Gutenberg-Richter law

As first step we calculated the b-value from the Gutenberg-Richter law (logN(M)=a-bM), which was achieved using the ZMAP matlab program extracted from the ETH Zurich (*Eidgenössische Technische Hochschule Zürich*) webpage. Zmap is a useful set of tools that allows as to analyze the data of seismic catalogs, calculate variable quantities and create seismicity maps. The ZMAP program is available at: http://www.seismo.ethz.ch/prod/software/zmap/index_EN.

The b-value was estimated by the maximum likelihood method (Pfanzagl 1994) in each one of the constracted subcatalogs. In order to achieve that we set a minimum magnitude and the program tries to make the best linear fit in a diagram of the logarithm of the cumulative number distribution to the magnitude of the earthquakes following the maximum likelihood estimation's principles. We did this for threshold magnitude 5, 5.5, 6, 6.5, 7, 7.5, 8, 8.5 and the results are shown in table 2.1.1 as well as examples of the graphs of the calculation. (The symbol "-" indicates that we did not have the appropriate number of events in order to estimate the b value in the specific time period). As an example, figures 2.1.1 to 2.1.8 present the calculation of b-value for period 1981-1985 for the threshold magnitudes setted each time. The GR relations for the other cases referred to table 2.1.1 are presented in Appendix 1.

M≥8.5	M≥8	M≥7.5	M≥7.0	M≥6.5	M≥6.0	M≥5.5	M≥5	years
-	-	2,08 ±0.08	1,68 ±0.06	1,43 ±0.10	1,31 ±0.10	1,21 ±0.11	1,12 ±0.15	1981-1985
-	-	1,79 ±0.08	1,56 ±0.06	1,32 ±0.08	1,26 ±0.08	1,18 ±0.09	1,1 ±0.12	1984-1988
-	-	2,40 ±0.09	1,87 ±0.11	1,48 ±0.13	1,36 ±0.14	1,25 ±0.15	1,15 ±0.17	1987-1991
-	-	1,53 ±0.24	1,59 ±0.19	1,43 ±0.17	1,31 ±0.17	1,24 ±0.17	1,17 ±0.17	1990-1994
-	1,50 ±0.08	1,82 ±0.07	1,27 ±0.13	1,17 ±0.12	1,11 ±0.11	1,08 ±0.10	1,05 ±0.10	1993-1997
-	3,01 ±0.00	2,05 ±0.07	1,35 ±0.14	1,18 ±0.13	1,10 ±0.12	1,07 ±0.11	1,05 ±0.11	1996-2000
-	0,90 ±0.090	1,47 ±0.1	1,33 ±0.1	1,15 ±0.11	1,10 ±0.11	1,07 ±0.10	1,05 ±0.10	1999-03
0,60 ±0.09	0,87 ±0.08	0,87 ±0.07	0,92 ±0.06	0,91 ±0.06	0,94 ±0.06	0,97 ±0.06	0,98 ±0.06	2002-2006
0,00	1,13 ±0.07	1,23 ±0.05	1,07 ±0.08	0,98 ±0.08	0,98 ±0.07	0,99 ±0.07	1,00 ±0.06	2005-2009
0,77 ±0.07	0,40 ±0.08	0,73 ±0.14	0,85 ±0.15	0,91 ±0.14	0,94 ±0.13	0,96 ±0.12	0,97 ±0.12	2008-2011

Table 2.1.1 : b values of the Gutenberg –Richter law for the global shallow seismicity

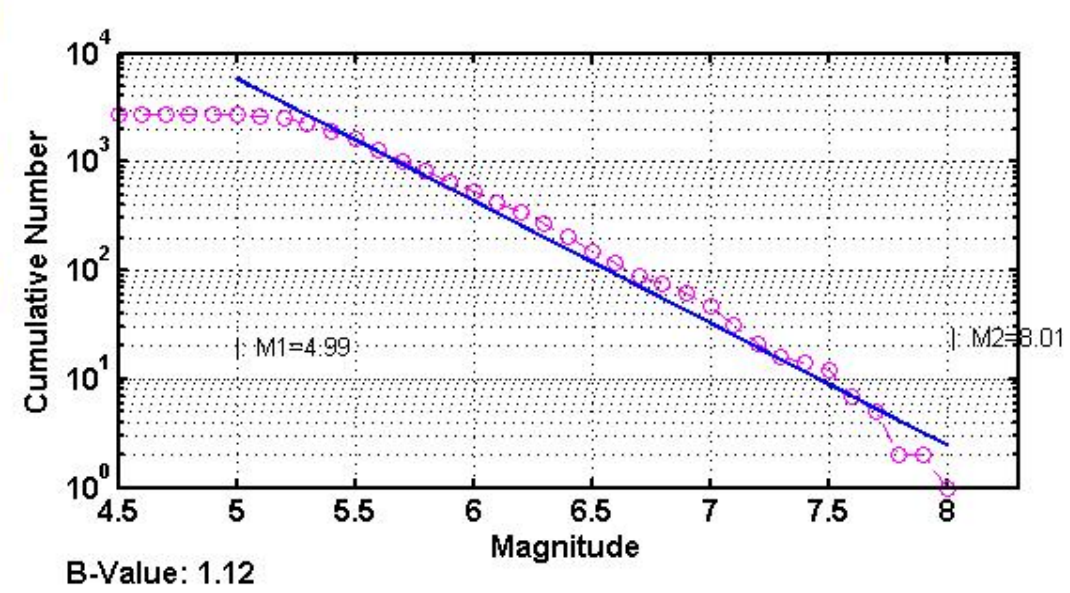

Figure 2.1.1: Example of calculation of the value b with Mw (min) = 5 (1981-1985)

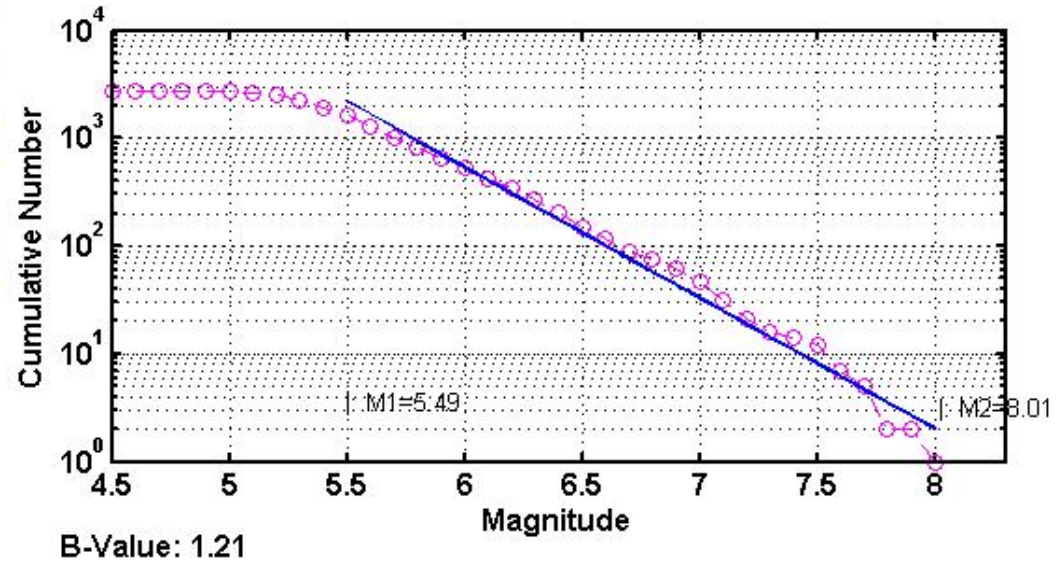

Figure 2.1.2: Example of calculation of the value b with Mw (min) = 5.5 (1981-1985)

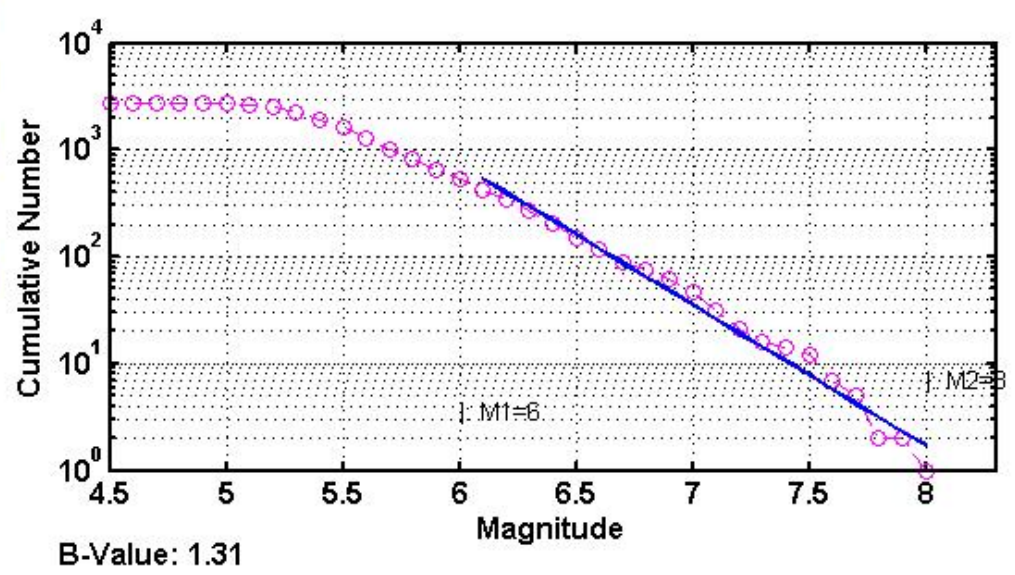

Figure 2.1.3: Example of calculation of the value b for Mw (min) =6 (1981-1985)

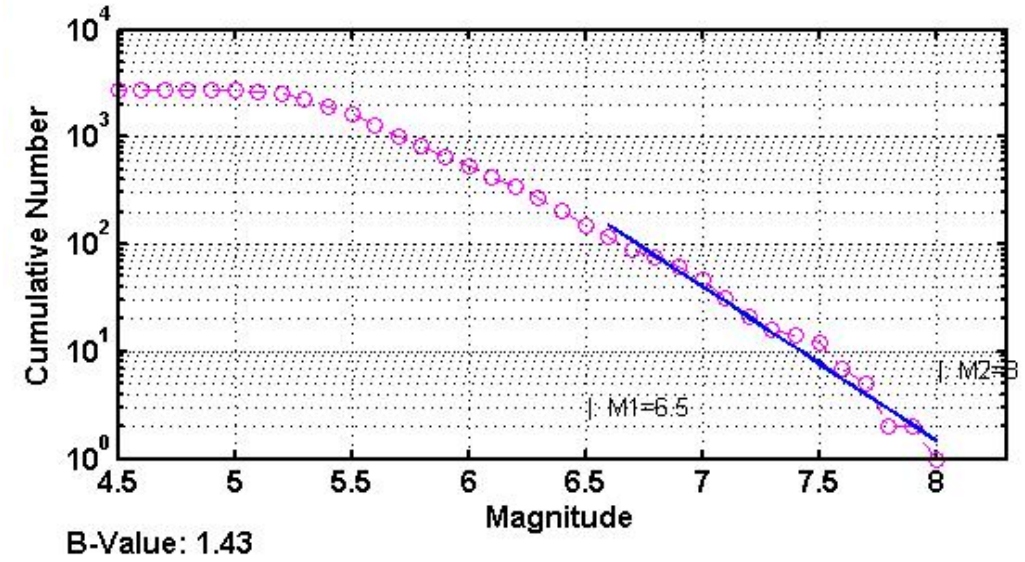

Figure 2.1.4: Example of calculation of the value b for Mw (min) =6.5 (1981-1985)

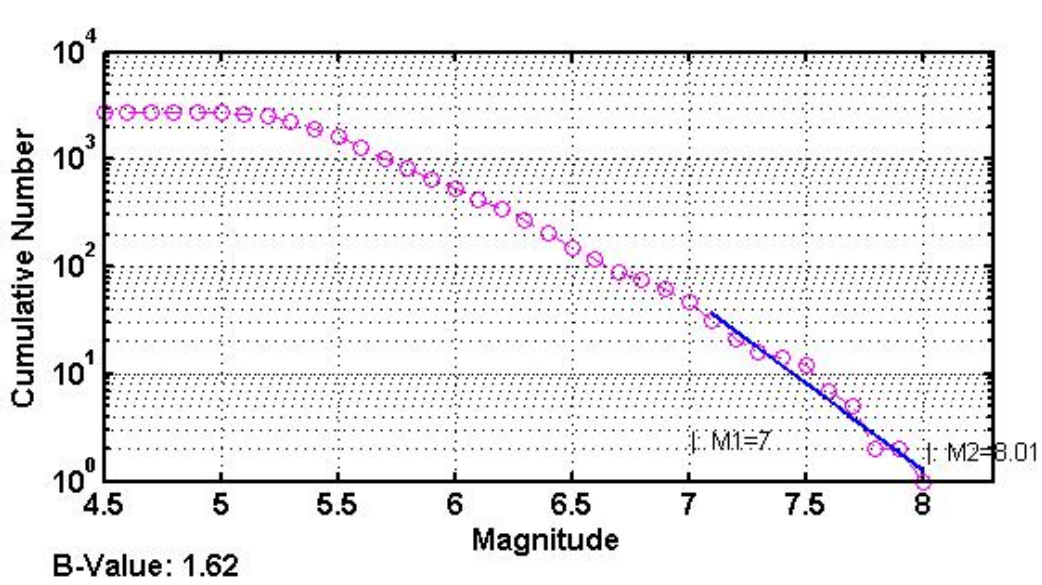

Figure 2.1.5: Example of calculation of the value b for Mw (min) = 7 (1981-1985)

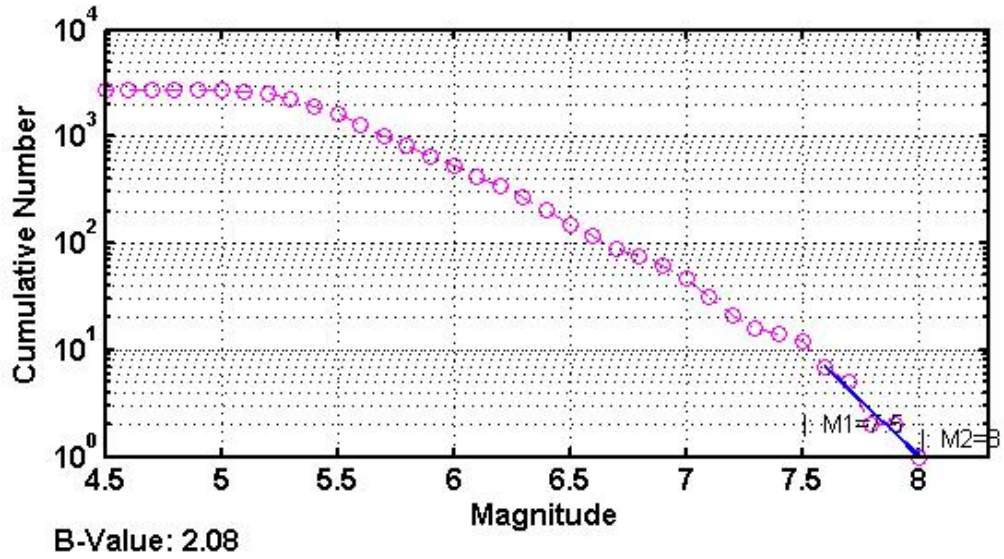

Figure 2.1.6: Example of calculation of the value b for Mw (min) = 7.5 (1981-1985)

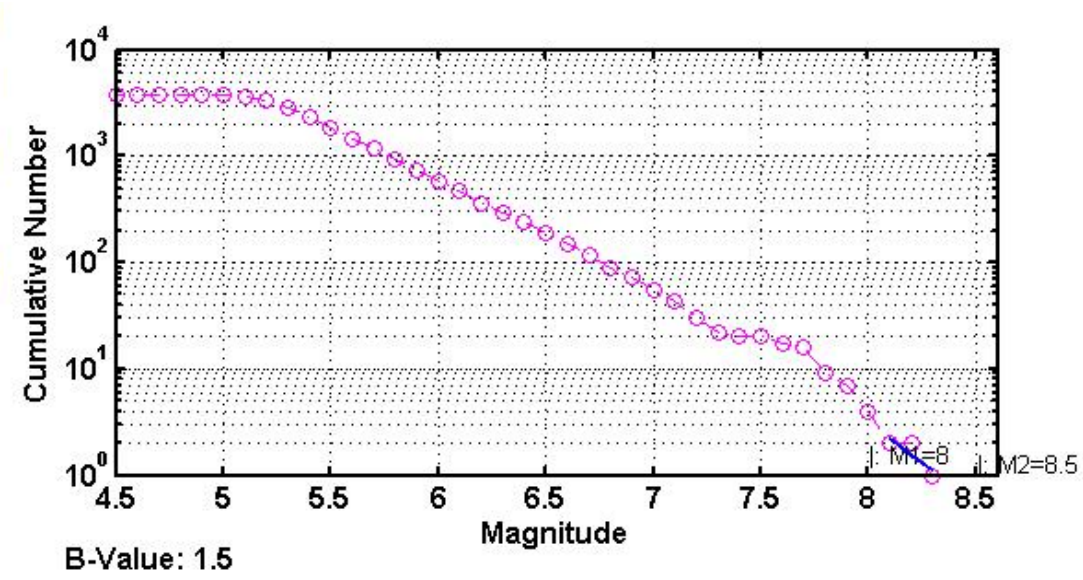

Figure 2.1.7: Example of calculation of the value b for Mw (min) = 8 (1981-1985)

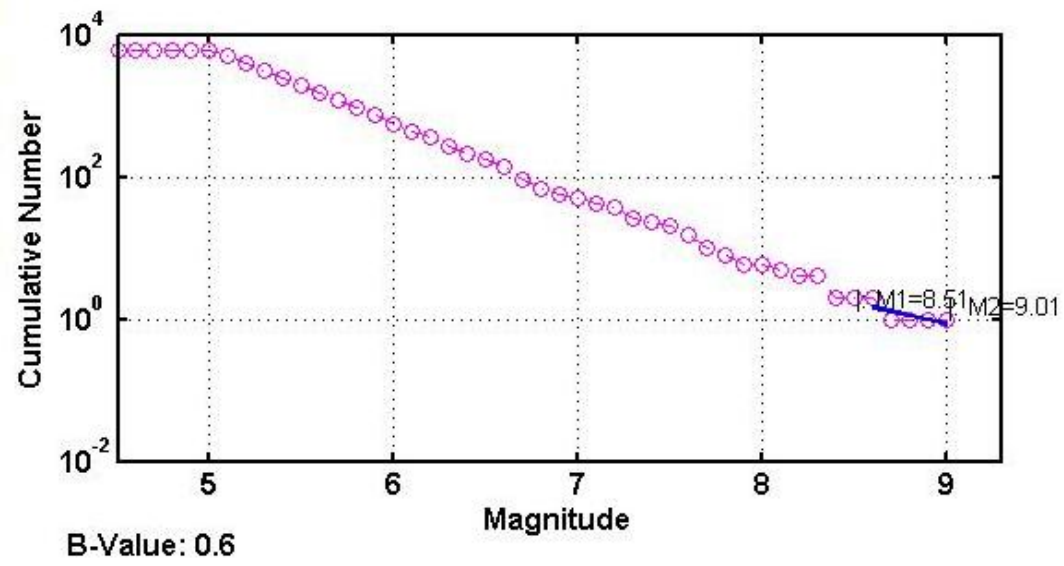

Figure 2.1.8: Example of calculation of the value b for Mw (min) = 8.5 (1981-1985)

2.2 The Nonextensive Model for Earthquake Frequency-Magnitude distribution

The Gutenberg–Richter (GR) law (Gutenberg and Richter, 1944) log-linearly relates the cumulative number of earthquakes with magnitude greater than M with the magnitude M_{th}. However, this is an empirical relationship that was not expressed from any principles of physics. Therefore, Sotolongo-Costa and Posadas (2004) proposed a model for earthquake generation mechanism, in which an energy distribution function was derived starting from first principles. The Sotolongo-Costa and Posadas (2004, SCP, hereafter) model considers as earthquake triggering mechanism the interaction between the asperities of the fault planes with the fragments between them, originated by the local breakage of the tectonic plates, from which the faults are generated. Based on the nonextensive Tsallis formalism (Tsallis,1988),a fragment size distribution is derived, which, combined with the roughness of the fault planes, leads to a mechanism of earthquake triggering. Two years later, Silva (2006) reinvestigated the above-mentioned method, developing a more realistic model, which assumes that the eventual relative position of fragments filling the space between two irregular faults can hinder their relative motion. Stress increases until a displacement of one of the asperities, due to the displacement of the hindering fragment, or even its breakage in the point of contact with the fragment leads to a relative displacement of the fault planes of the order of the size ρ of the hindering fragment, with the subsequent energy release E (Sotolongo-Costa and Posadas, 2004). Because large fragments are more difficult to release than small ones, the energy scales as $\varepsilon \sim \rho^3$, in agreement with the scaling relationship between seismic moment and the product of the fault rupture area with the average displacement of the fault (Lay and Wallace, 1995). Such relationship differs from that given by Sotolongo-Costa and Posadas (2004), where $E \sim \rho$, leading to a difference in the estimate of the parameter a, which is the proportionality constant of each of the proposed relationships.

Starting from the main principle of maximization of the Tsallis entropy (Tsallis, 1988) we take:

$$S_q = k\frac{1-\int P_\sigma^q(\sigma)d\sigma}{q-1} \qquad (2.1)$$

we derive the expressions (2.9) and (2.10) as described in section 1.3:

$$\frac{N(>M)}{N} = \left[1-\left(\frac{1-q}{2-q}\right)\left(\frac{10^M}{a^{\frac{2}{3}}}\right)\right]^{\frac{2-q}{1-q}} \qquad (2.2)$$

$$\frac{N(>M)}{N} = \left[\frac{1-\left(\frac{1-q}{2-q}\right)\left(\frac{10^M}{a^{\frac{2}{3}}}\right)}{1-\left(\frac{1-q}{2-q}\right)\left(\frac{10^{Mo}}{a^{\frac{2}{3}}}\right)}\right]^{\frac{2-q}{1-q}} \qquad (2.3)$$

We have applied the non-extensive model of the last equation to the magnitude distribution of the earthquake activity of the whole catalog and the results are summarized in table 2.2.1:

Years	q_M
1981-1985	1,4211
1984-1988	1,4342
1987-1991	1,4160
1990-1994	1,4253
1993-1997	1,4686
1996-2000	1,4727
1999-2003	1,4746
2002-2006	1,4848
2005-2009	1,4695
2008-2011	1,4760

Table 2.2.1: The entropic index q_M for the global catalog with events with magnitude Mw≥5.0 and depth H≤150 km.

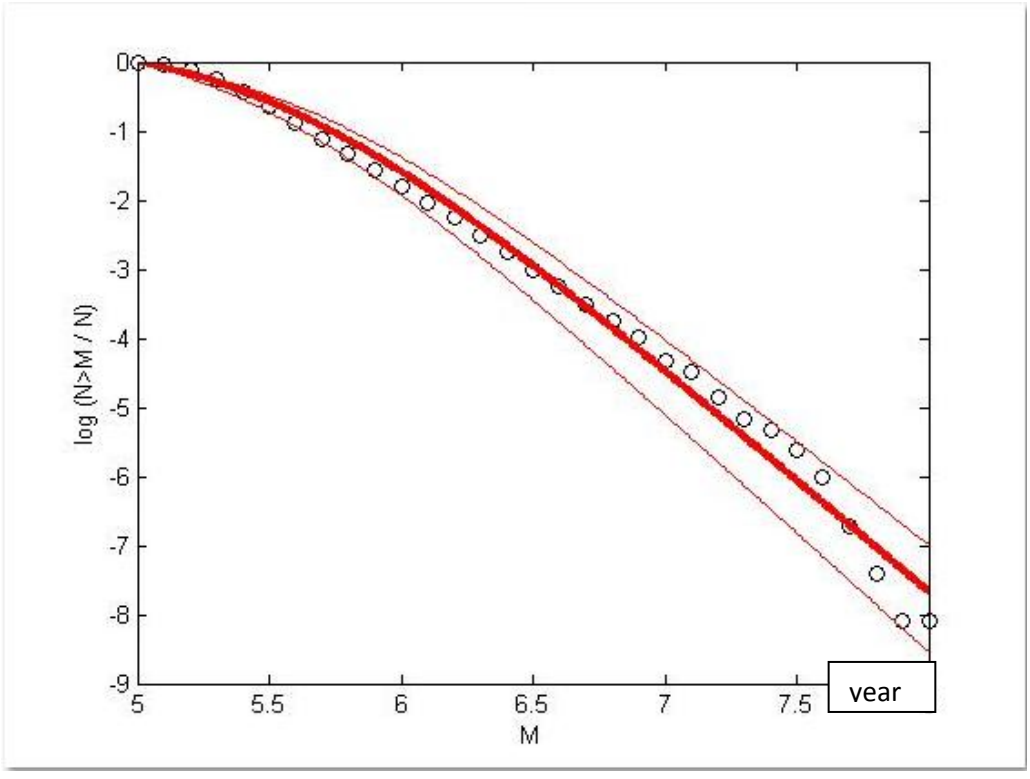

Figure 2.2.1: The magnitude-frequency distribution of earthquakes along with fitting based in eq (2.10) with q=1.421. The lines represent the 95% confidence error (1981-1985)

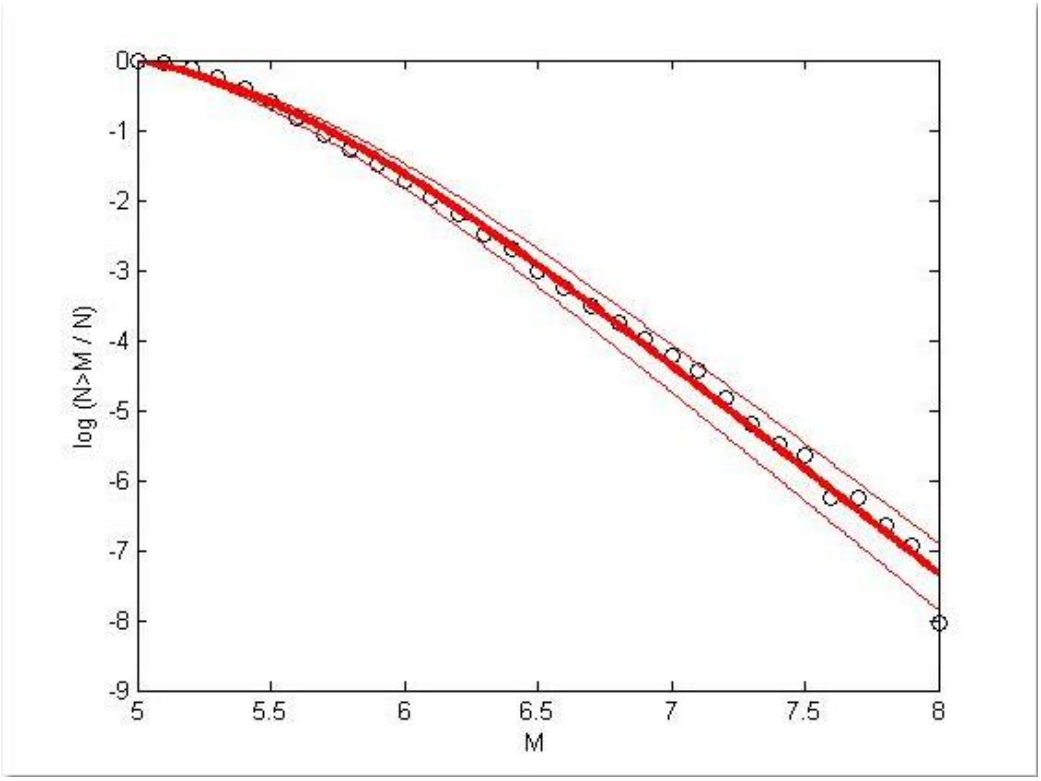

Figure 2.2.2: The magnitude-frequency distribution of earthquakes along with fitting based in eq (2.10) with q=1.434. The lines represent the 95% confidence error (1984-1988)

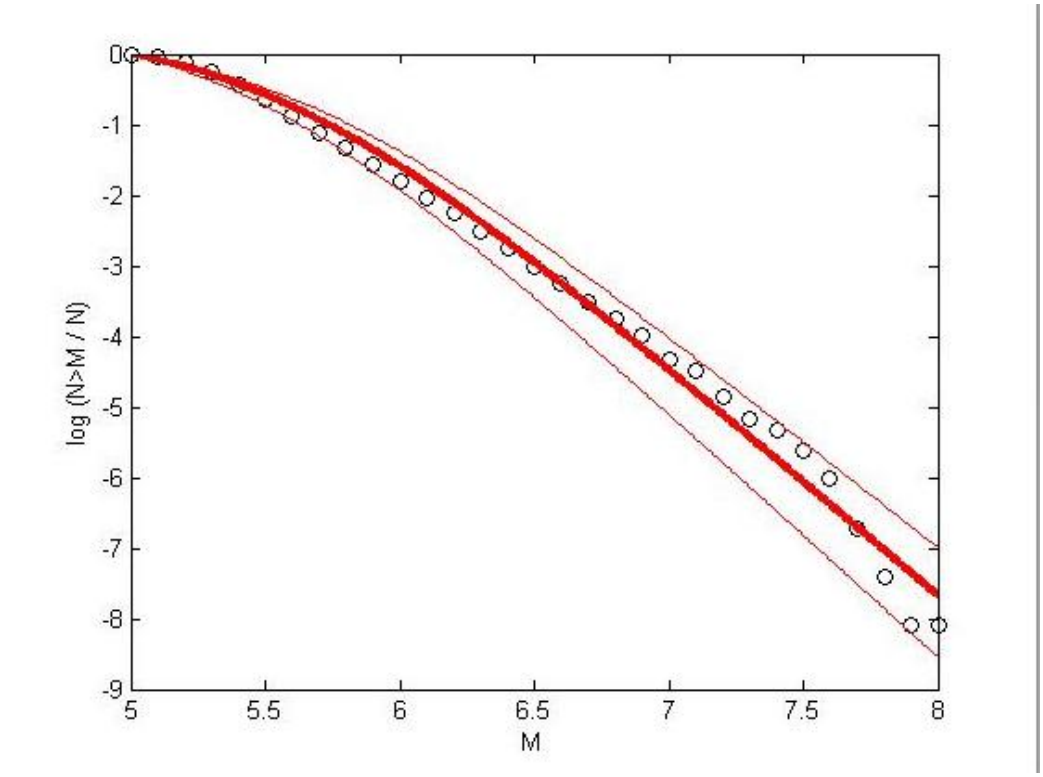

Figure 2.2.3: The magnitude-frequency distribution of earthquakes along with fitting based in eq (2.10) with q=1.416. The lines represent the 95% confidence error (1987-1991)

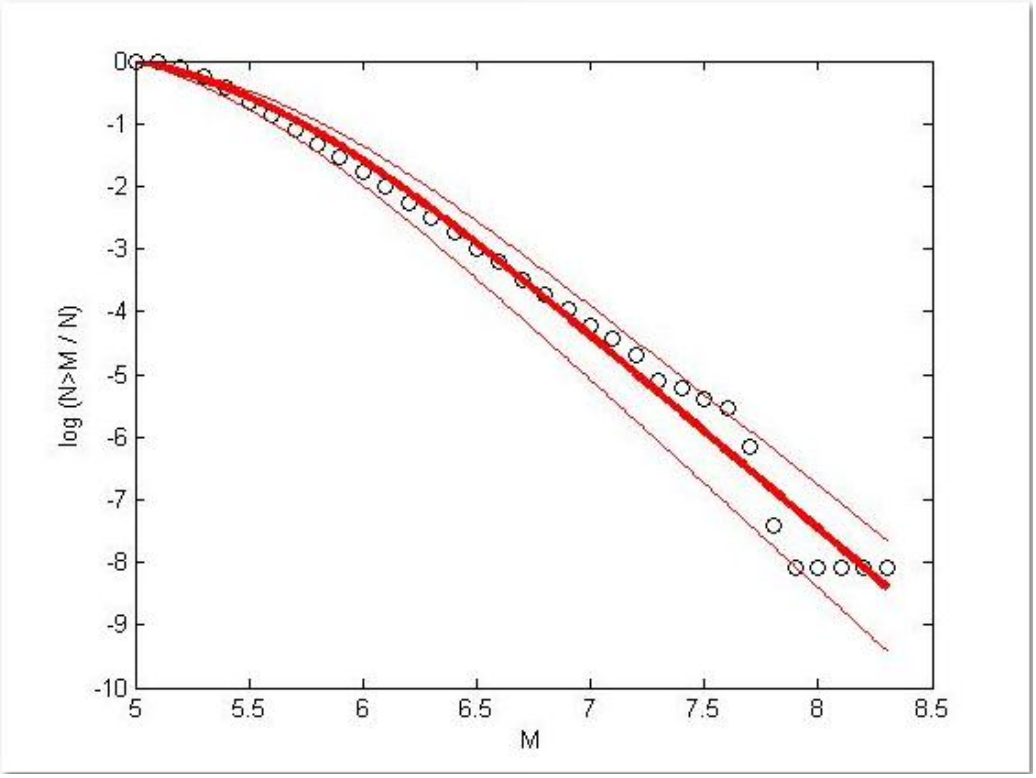

Figure 2.2.4: The magnitude-frequency distribution of earthquakes along with fitting based in eq (2.10) with q=1.425. The lines represent the 95% confidence error (1990-1994)

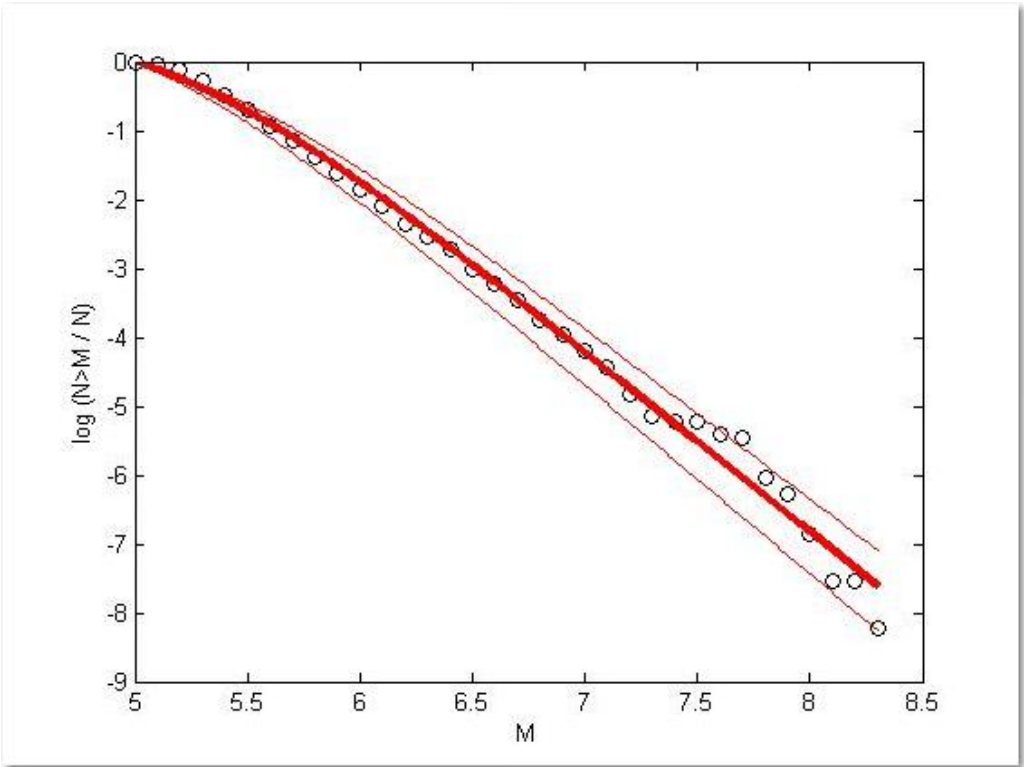

Figure 2.2.5: The magnitude-frequency distribution of earthquakes along with fitting based in eq (2.10) with q=1.467. The lines represent the 95% confidence error (1993-1997)

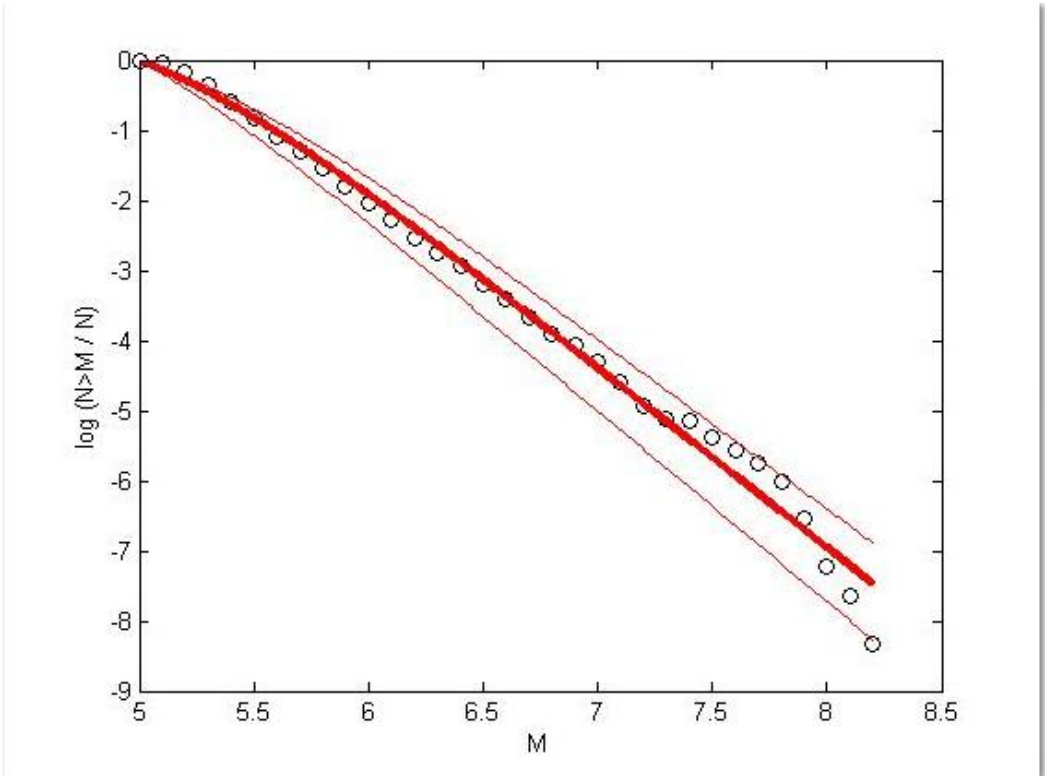

Figure 2.2.6: The magnitude-frequency distribution of earthquakes along with fitting based in eq (2.10) with q=1.473. The lines represent the 95% confidence error (1996-2000)

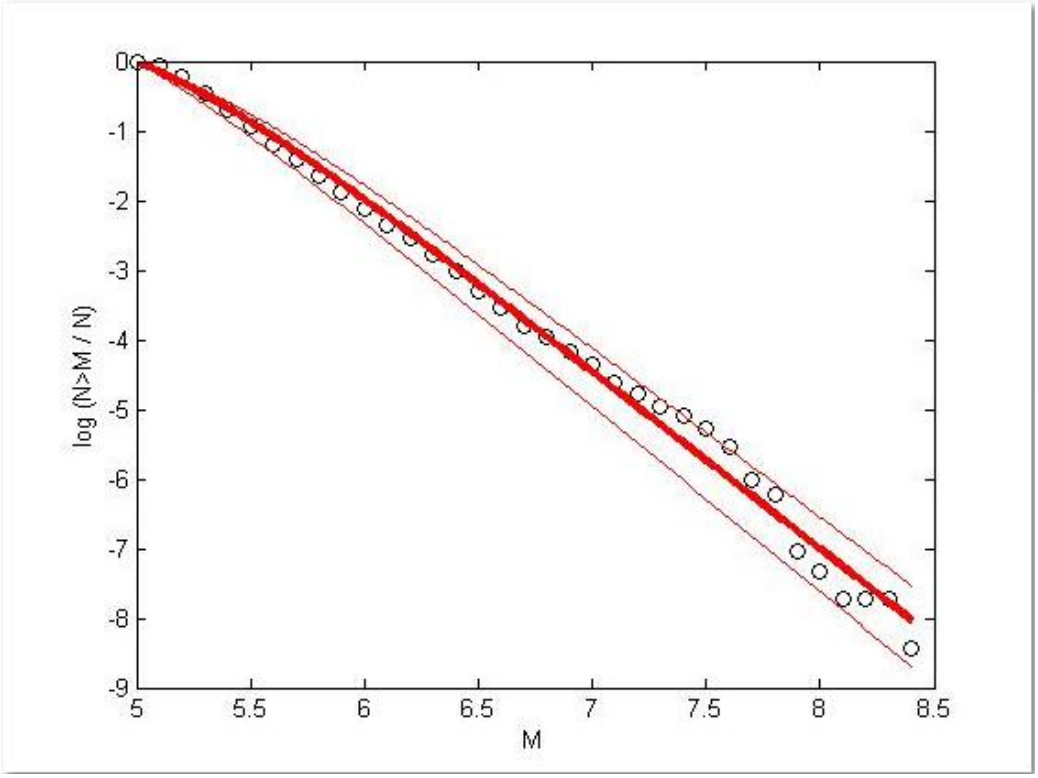

Figure 2.2.7: The magnitude-frequency distribution of earthquakes along with fitting based in eq (2.10) with q=1.475. The lines represent the 95% confidence error (1999-2003)

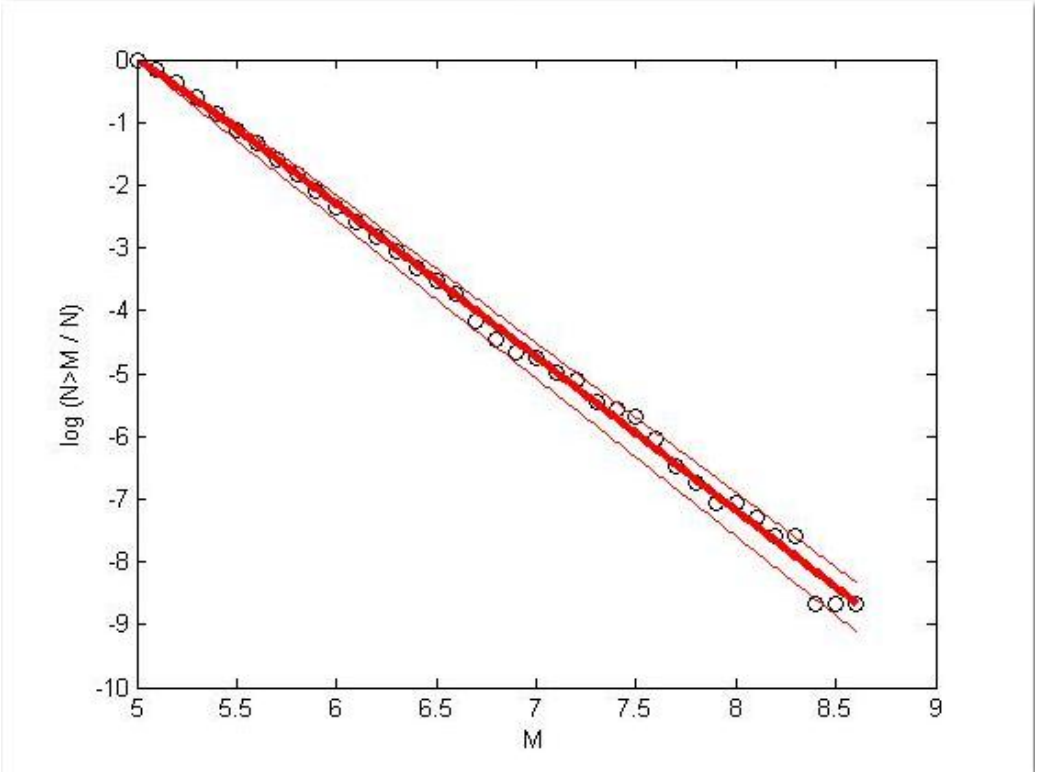

Figure 2.2.8: The magnitude-frequency distribution of earthquakes along with fitting based in eq (2.10) with q=1.485. The lines represent the 95% confidence error (2002-2006)

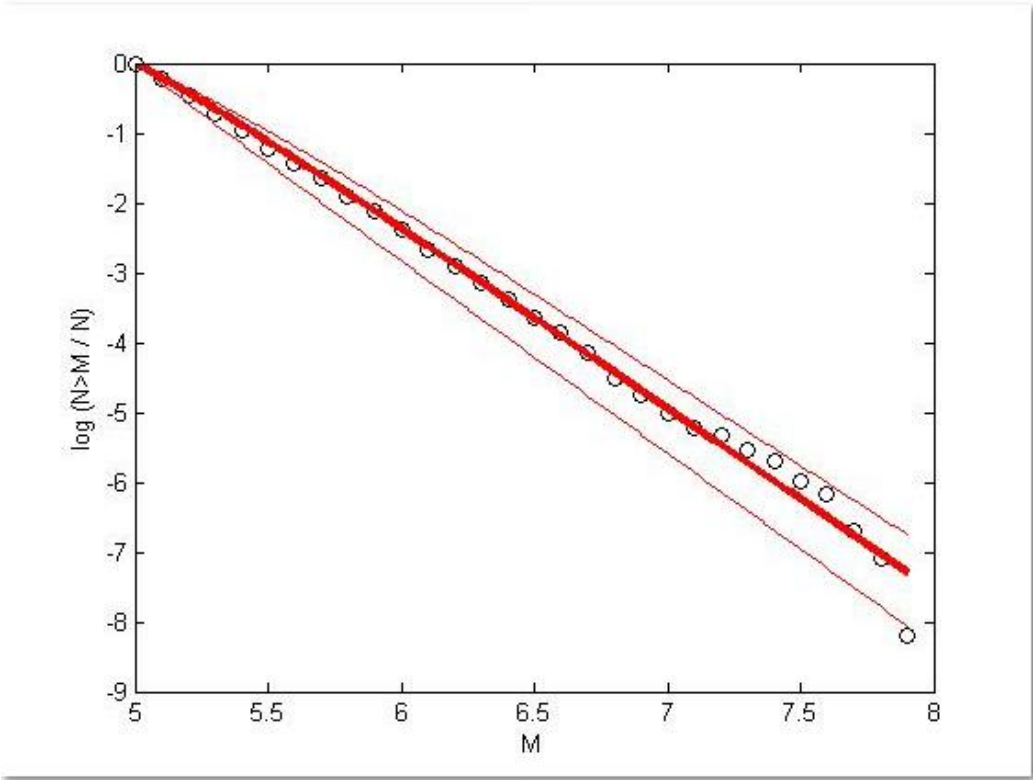

Figure 2.2.9: The magnitude-frequency distribution of earthquakes along with fitting based in eq (2.10) with q=1.470. The lines represent the 95% confidence error (2005-2009)

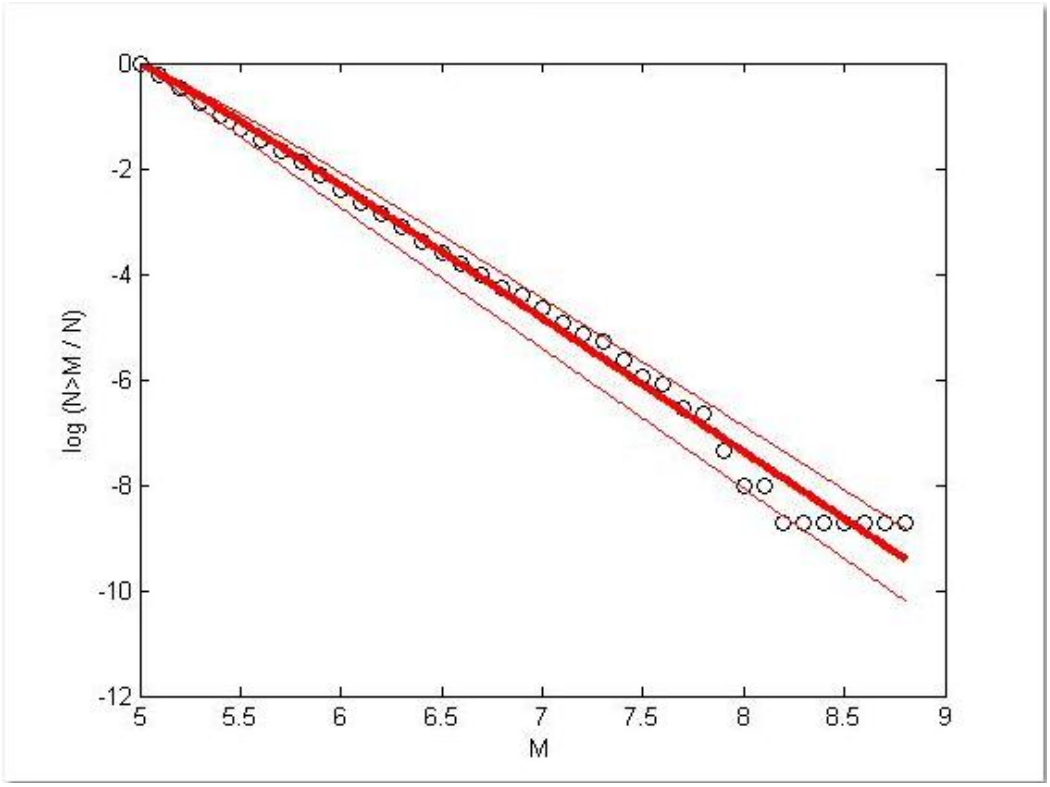

Figure 2.2.10: The magnitude-frequency distribution of earthquakes along with fitting based in eq (2.10) with q_M=1.476. The lines represent the 95% confidence error (2008-2011)

2.3 The frequency-magnitude distribution for the regionalized catalog

To integrate our search there is an obvious need to estimate the entropic index q_M, as well as the b-value from the Gutenberg-Richter law inside these regions, in order to reach a conclusion.

Following the same procedure, described in chapter 2.2 for the magnitude distribution for the regionalized catalog that contains earthquakes with magnitude equal or greater than Mw=5 we take the results shown in table 2.3.1.

Region	q_M
Region 1	1,491
Region 2* (2-3-4)	1,418
Region 5	1,498
Region 6	1,470
Region 7	1,474
Region 8	1,516
Region 9	1,195
Region 10	1,421
Region 11	1,555
Region 12	1,471
Region 13	1,295
Region 14*(14-15)	1,424
Region 16	1,463
Region 17*(17-18)	1,472
Region 19*(19-20-21)	1,507
Region 22*(22-23)	1,425
Region 24	1,493
Region 25*(25-26-27-28-47)	1,494
Region 29	1,466
Region 30	1,429
Region 31	1,368
Region 32	1,354
Region 33	1,459
Region 34	-
Region 35	-
Region 36	-
Region 37	1,481
Region 38	-
Region 39	1,429
Region 40	1,346
Region 41	1,267
Region 42	1,470
Region 43	1,285
Region 44	1,184

Region 45	1,267
Region 46	1,470
Region 48	1.482
Region 49	-
Region 50	-

Table 2.3.1: The entropic index q_M for the regionalized catalog with events with magnitude Mw≥5.0 and depth H≤150 km.

Finally, the calculation of the Gutenberg-Richter's law gives as the following b-values for the F-E regions:

	b value	No events
Region 1	0,96	1135
Region 2* (2-3-4)	0,99	517
Region 5	1	674
Region 6	1,06	559
Region 7	0,79	283
Region 8	1,03	1608
Region 9	1,18	105
Region 10	1,07	660
Region 11	0,81	323
Region 12	0,89	2392
Region 13	1,19	299
Region 14*(14-15)	1,03	3361
Region 16	1	1097
Region 17*(17-18)	1,08	872
Region 19*(19-20-21)	0,95	3006
Region 22*(22-23)	1,13	2372
Region 24	0,85	1265
Region 25*(25-26-27-28-47)	0,91	822
Region 29	0,97	313
Region 30	1,03	377
Region 31	1,31	160
Region 32	1,36	1268
Region 33	1,23	1104
Region 34	1,03	40
Region 35	-	2
Region 36	1,65	14
Region 37	0,96	271
Region 38	1,12	23
Region 39	0,92	90
Region 40	1,28	230
Region 41	1,03	62

Region 42	0,69	74
Region 43	1,7	1052
Region 44	1,67	230
Region 45	1,33	315
Region 46	0,84	963
Region 48	1,11	200
Region 49	-	0
Region 50	-	4

Table 2.3.2: b values of the Gutenberg-Richter law for the regionalized catalog with events with magnitude Mw≥5 and depth H≤150 km.

Starting from equation 2.2 and considering that the GR law is given by the expression: logN(M)=a-bM, we can easily derive, after some algebra, the relationship:

$$b=\frac{2-q_M}{q_{M-1}} \qquad (2.4)$$

, that connects the b value with the entropic index q_M. The table that follows presents the b-value estimated from equation 2.4 inside the FE regions, while the b value calculated from the GR law can be found in table 2.3.2.

	$b=\frac{2-q_M}{q_M-1}$
Region 1	1.04
Region 2* (2-3-4)	1.39
Region 5	1.01
Region 6	1.13
Region 7	1.11
Region 8	0.94
Region 9	4.13
Region 10	1.38
Region 11	0.80
Region 12	1.12
Region 13	2.39
Region 14*(14-15)	1.36
Region 16	1.16
Region 17*(17-18)	1.12
Region 19*(19-20-21)	0.97
Region 22*(22-23)	1.35
Region 24	1.03
Region 25*(25-26-27-28-47)	1.02
Region 29	1.15
Region 30	1.33
Region 31	1.72
Region 32	1.83
Region 33	1.18
Region 34	-
Region 35	-

Region 36	-
Region 37	1.08
Region 38	-
Region 39	1.33
Region 40	1.89
Region 41	2.75
Region 42	1.13
Region 43	2.51
Region 44	4.44
Region 45	2.75
Region 46	1.13
Region 48	1.08
Region 49	-
Region 50	-

Table 2.3.3: The b value estimated from eq. 2.4 inside the FE regions

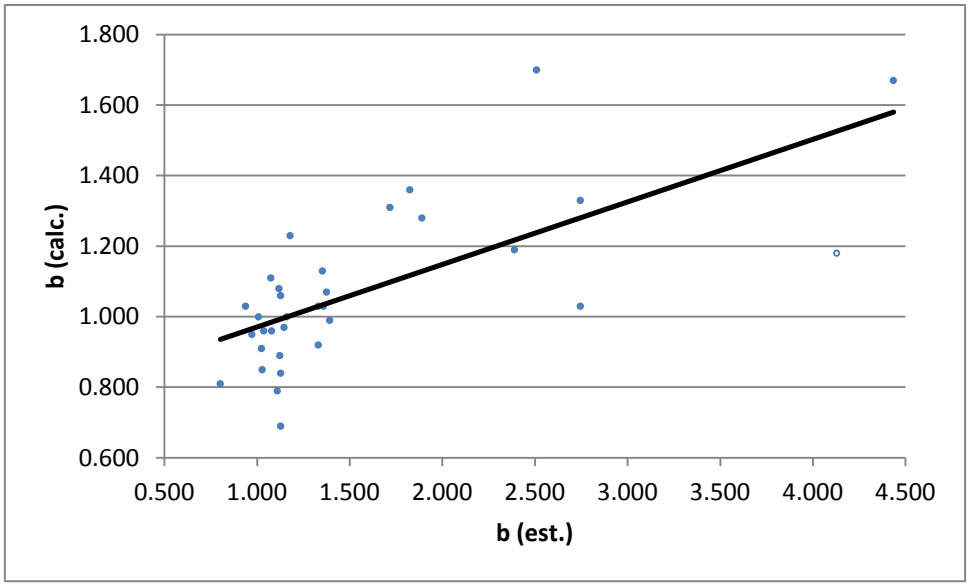

Figure 2.3.1: linear fitting between the b value calculated from the GR law (vertical axis) and the b value estimated from eq. 2.4 (horizontal axis).

2.4 The interevent times

In the whole 30-year worldwide seismicity catalog that we are using for our study there are in total 28138 seismic events (N_o=28138). We successively calculated the interevent time between all successive earthquakes and created a catalog, which describes the number of earthquakes with inter-event time equal or greater than T. By dividing the number of earthquakes with inter-event time equal or greater than T with the total number of seismic events we take the probability of occurrence of an earthquake with inter-event time equal or greater than T. We repeated the procedure for all the subcatalogs analysed. The results are presented in figures 2.4.1 to 2.4.11.

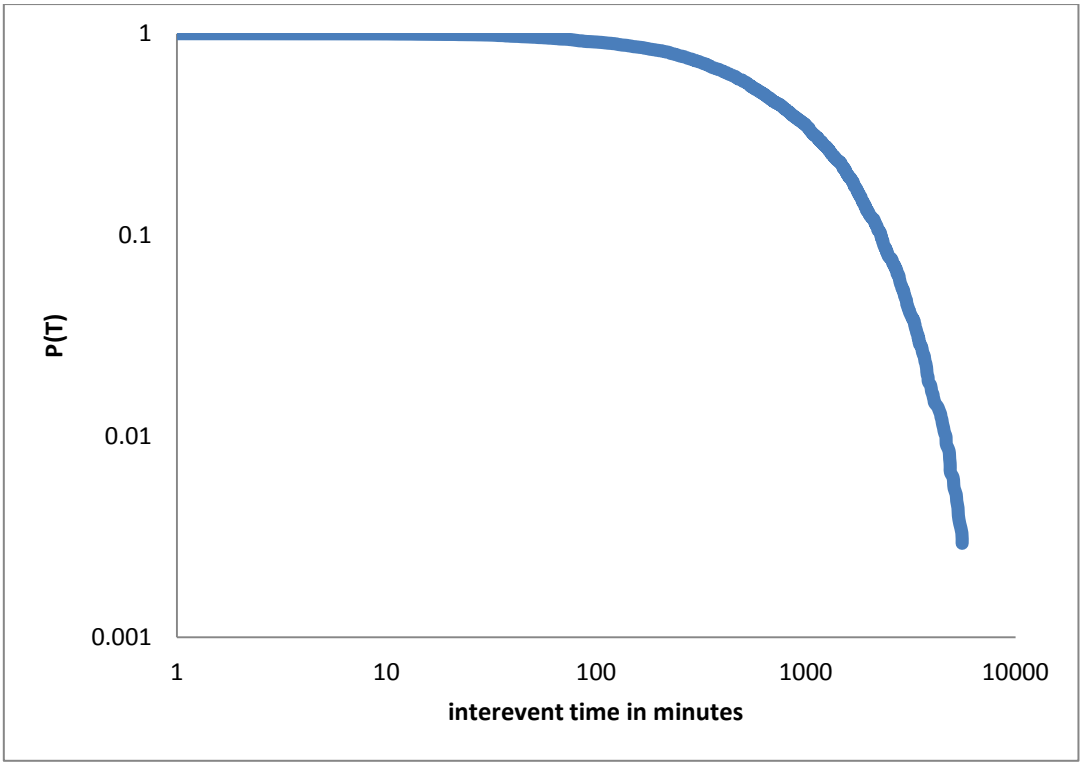

Figure 2.4.1 : The interevent time probability distribution for years 1981-1985

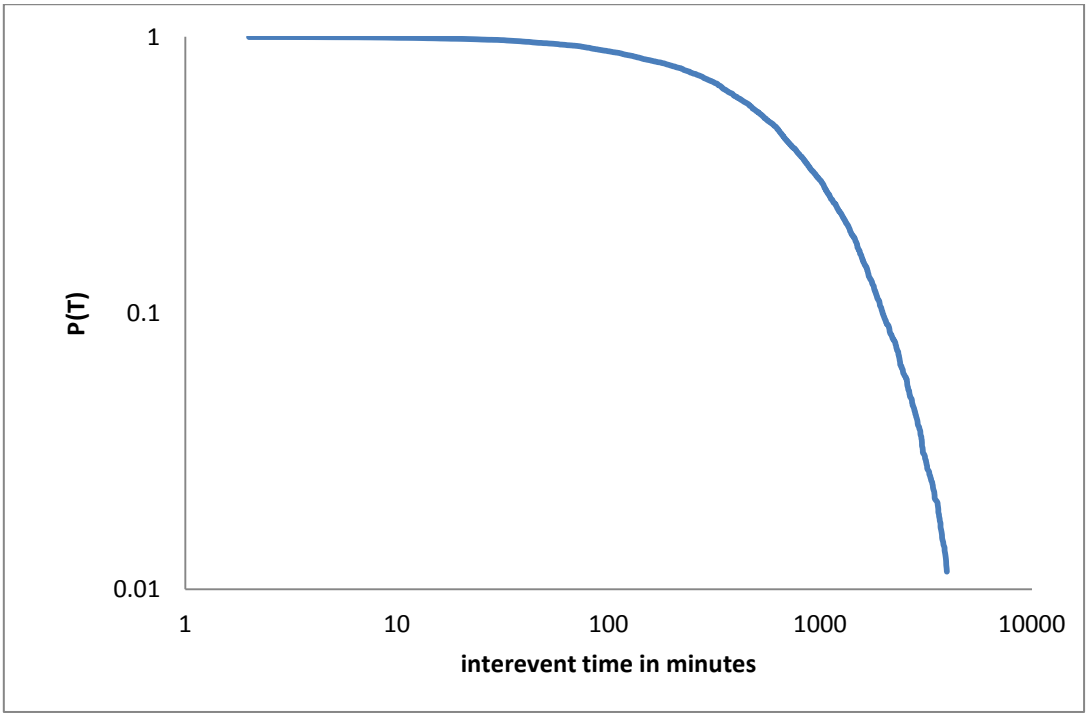

Figure 2.4.2 : The interevent time probability distribution for years 1984-1988

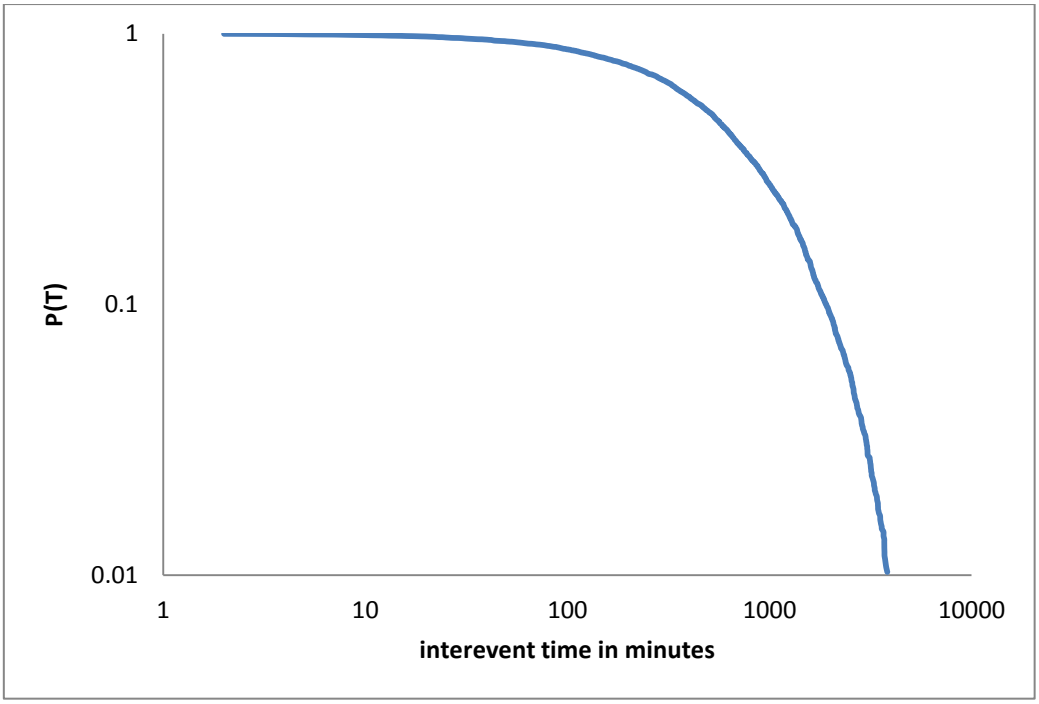

Figure 2.4.3 : The interevent time probability distribution for years 1987-1991

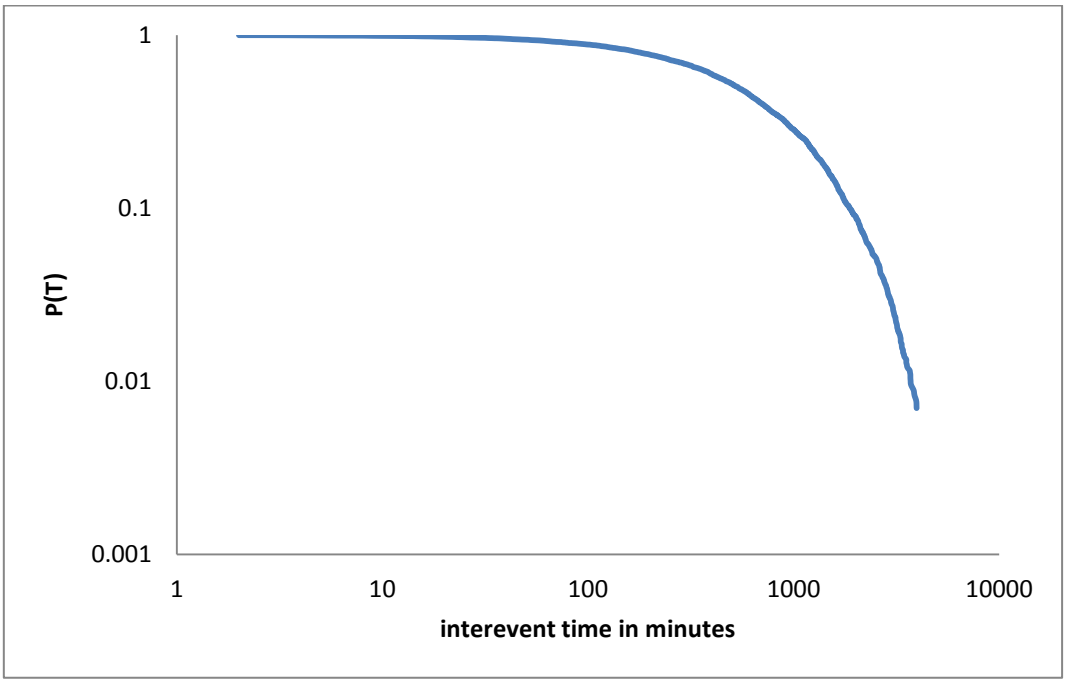

Figure 2.4.4 : The interevent time probability distribution for years 1990-1994

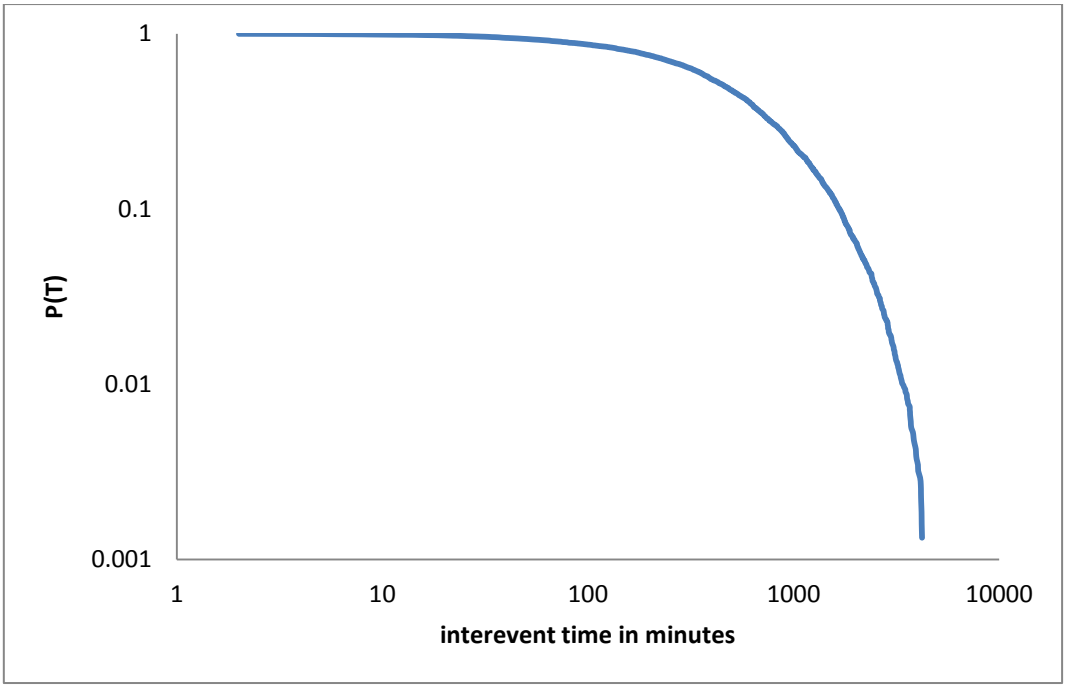

Figure 2.4.5: The interevent time probability distribution for years 1993-1997

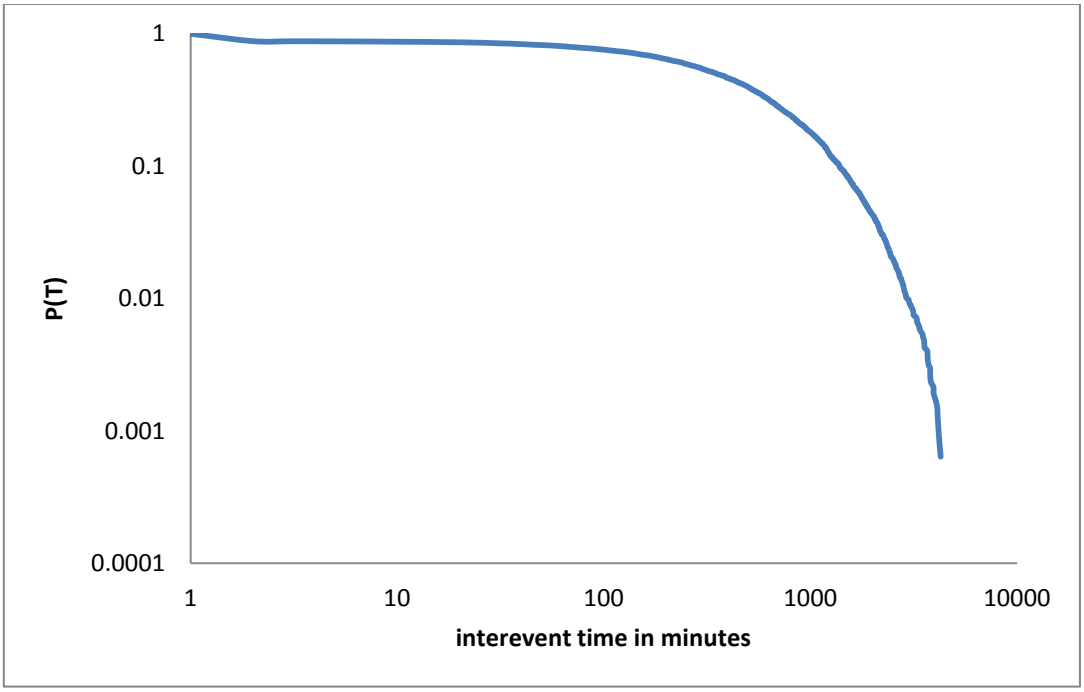

Figure 2.4.6 : The interevent time probability distribution for years 1996-2000

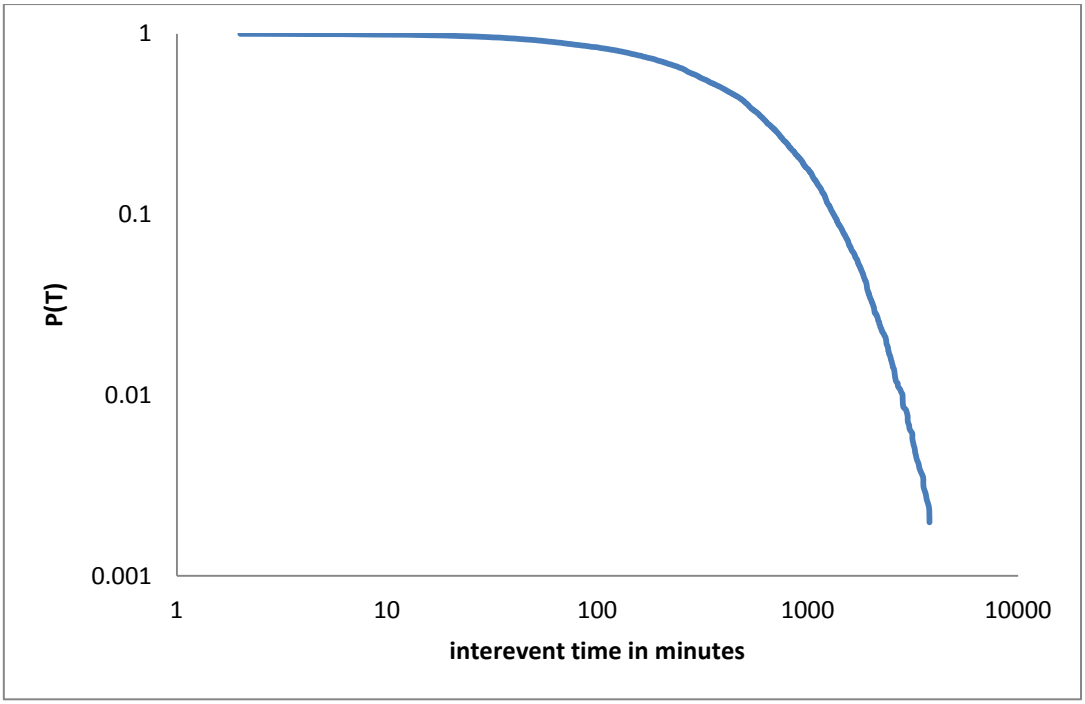

Figure 2.4.7 : The interevent time probability distribution for years 1999-2003

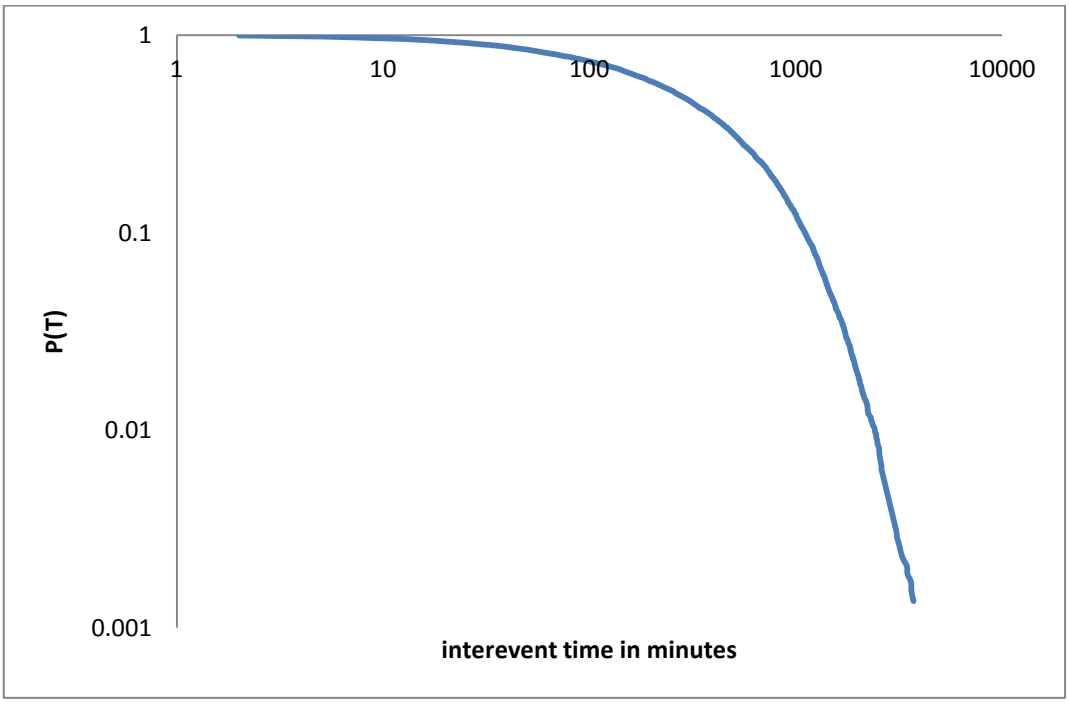

Figure 2.4.8: The interevent time probability distribution for years 2002-2006

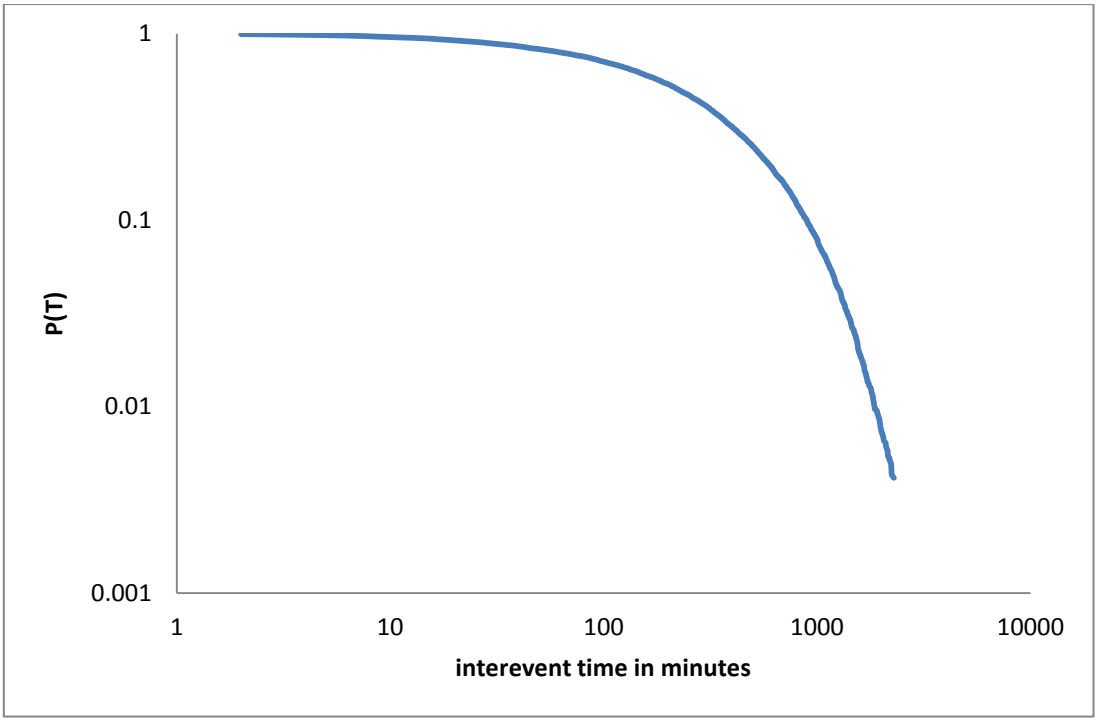

Figure 2.3.4.9 : The interevent time probability distribution for years 2005-2009

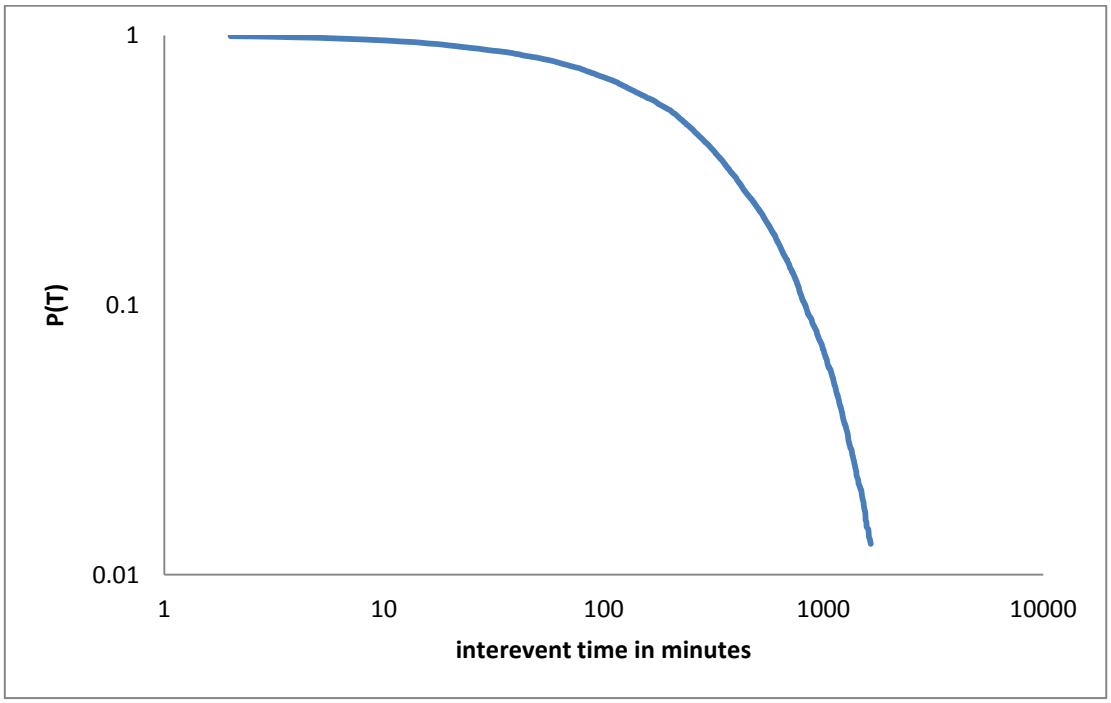

Figure 2.4.10: The interevent time probability distribution for years 2008-2011

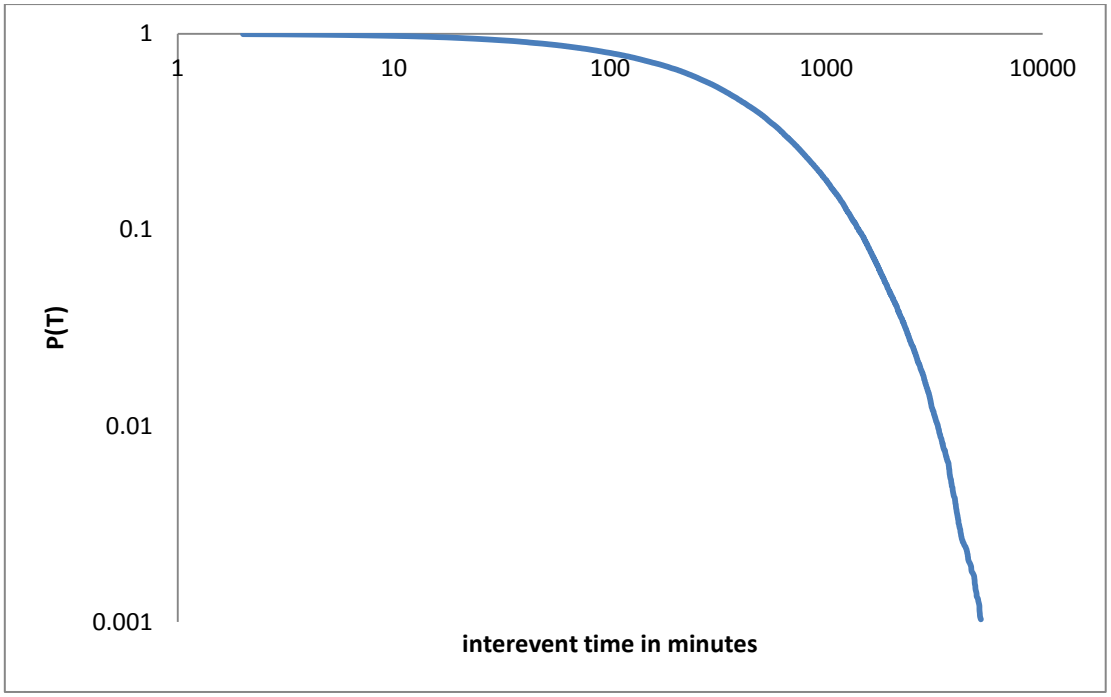

Figure 2.4.11: The interevent time probability distribution for the whole catalog of global seismicity within the period of 1/01/1981 to 31/12/2011.

An important point to non-extensive analysis is that the quantity to be compared with the observed distribution is the associated escort distribution (Tsallis 2009, Abe and Suzuki 2003, 2005). Following the latter approach, the cumulative distribution function is given by the expression:

$$P(>T) = \int_0^{\infty} P_q(T)dT \qquad (2.4)$$

where :

$$P_q(T) = \frac{P^q(T)}{\int_0^{\infty} P^q(T)dT} \qquad (2.5)$$

and combining with the probability function

$$p(T)=\frac{[1-(1-q)BT]^{1/(1-q)}}{Z_q} = \frac{\exp_q(-BT)}{Z_q} \qquad (2.6)$$

we obtain $P(>T) = \exp_q(-BT)$. This implies that after the estimation of the appropriate q that describes the observed distribution for P(>T) the q-logarithmic function lnq (P(>T)) anexpressed as

$$\ln_q(T)\frac{1}{1-q}(T^{1-q}-1) \qquad (2.7)$$

is approximately linear with T (Vallianatos 2011).

2.4.1 Analysis of global shallow seismicity.

Following the latter approach, the analisis of the inter-event time distributions gives us the semi-q-log plot of the cumulative distribution for the inter-event times, where the straight line represents the q-logarithmic function described earlier. Our results are presented in table 2.4.1.1 and graphs that follow (see figure 2.4.1.1, 2.4.1.2)

	q_T	cor.coeff.
1981-1985	1,046	-0,9994
1984-1988	1,030	-0,9995
1987-1991	1,033	-0,9992
1990-1994	1,035	-0,998
1993-1997	1,026	-0,9984
1996-2000	1,025	-0,9989
1999-2003	1,010	-0,9994
2002-2006	1,049	-0,9992
2005-2009	1,063	-0,9953
2008-2011	1,062	-0,9984
1981-2011	1,031	-0,9702

Table 2.4.1.1 : The q_T parameter after the analysis of the global catalog with events with magnitude Mw≥5.0 and depth 0-150km

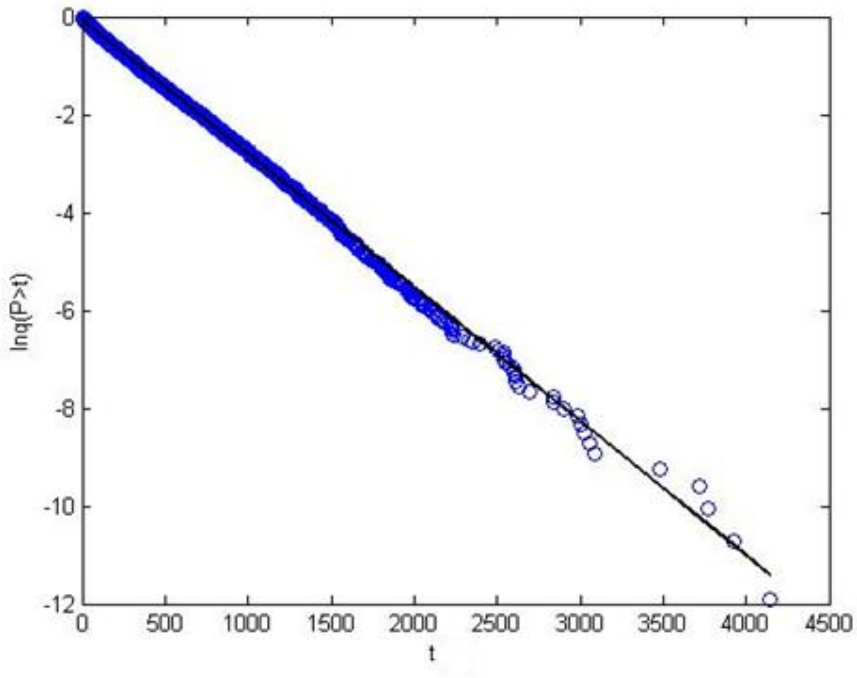

Figure 2.4.1.1: The semi-q-plot of the cumulative distribution for the interevent times for the data set of period 2005-2009 with earthquakes with magnitude equal or greater than the threshold magnitude Mw=5.0 and depth H≤150km. The straight line represents the q-logarithmic function with value q_T=1.063

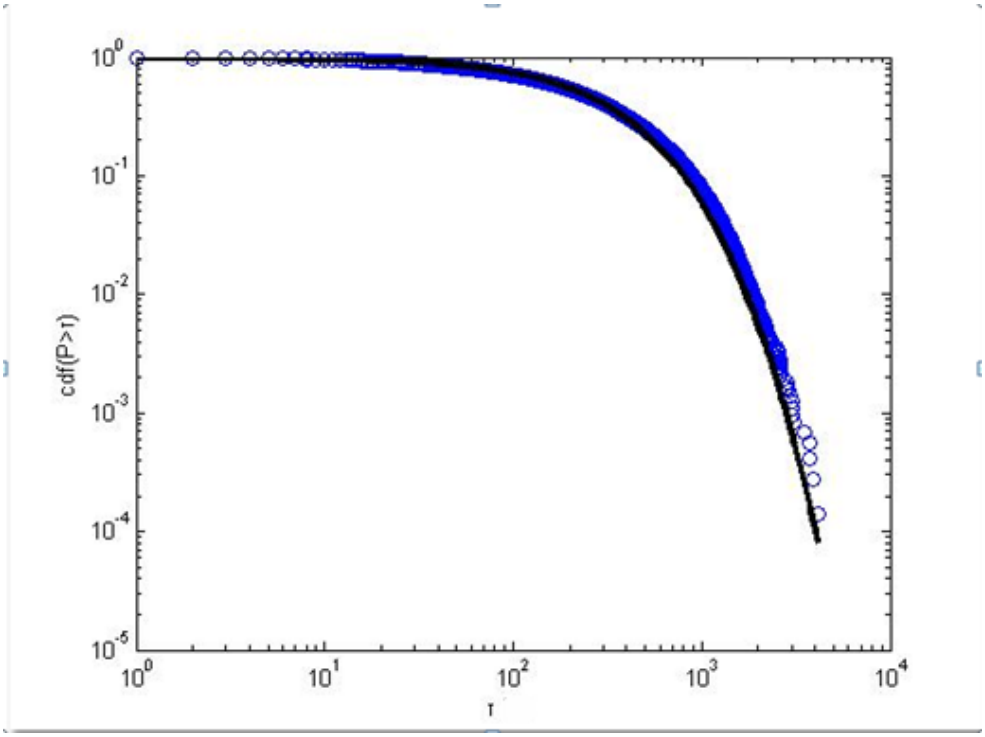

Figure 2.4.1.2:The cumulative distribution for the interevent times for the data set of period 2005-2009 with earthquakes with magnitude equal or greater than the threshold magnitude Mw=5.0 and depth H≤150 km. The value of the logarithmic function q_T is 1.063.

Our results for the initial unmodified global catalog indicate that the value "q_T" is close to 1 and the dependence of the worldwide events is negligible**.** Trying to find a dependence between the times that the earthquakes occur , we have created new seismic catalogs which contain only the events with magnitude greater or equal to Mw=5.5, Mw=6 , both with maximum depth 150 km, as well as a catalog with earthquakes with magnitude equal or greater that Mw=5.0 and depth H≤50 km and, as described above, we fitted the interevent times distribution using the q-exponential function. The results that came out are shown in tables 2.4.1.2, 2.4.1.3, 2.4.1.3:

	q	**cor. Coeff**
1981-1985	1,029	-0,999
1984-1988	1,089	-0,998
1987-1991	1,102	-0,998
1990-1994	1,048	-0,999
1993-1997	1,054	-0,998
1996-2000	1,075	-0,999
1999-2003	1,080	-0,999
2002-2006	1,038	-0,999
2005-2009	1,060	-0,999
2008-2011	1,058	-0,999
1981-2011	1,055	-0,999

Table 2.4.1.2 :The q_T parameter after the analysis of the global catalog with events with magnitude Mw≥5.5 and depth H≤150 km.

	q	cor.coeff
1981-1985	1,023	-0,998
1984-1988	1,07	-0,998
1987-1991	1,07	-0,998
1990-1994	1,051	-0,999
1993-1997	1,017	-0,999
1996-2000	1,02	-0,996
1999-2003	1,001	-0,996
2002-2006	1,001	-0,995
2005-2009	1,018	-0,999
2008-2011	1,091	-0,998
1981-2011	1,008	-0,999

Table 2.4.1.3 : The q_T parameter after the analysis of the global catalog with events with magnitude Mw≥6.0 and depth H≤150km.

	q	cor. Coeff
1981-1985	1,001	-0,992
1984-1988	1,001	-0,991
1987-1991	1,001	-0,996
1990-1994	1,001	-0,994
1993-1997	1,001	-0,991
1996-2000	1,001	-0,994
1999-2003	1,001	-0,984
2002-2006	1,018	-0,996
2005-2009	1,056	-0,992
2008-2011	1,001	-0,994
1981-2011	1,001	-0,995

Table 2.4.1.4 : The q_T parameter after the analysis of the global catalog with events with magnitude Mw≥5.0 and depth 0-50km.

2.4.2 Analysis of seismicity in Flinn-engdahl regions based on Tsallis entropy.

Our next step was to divide the globe into geographical regions according to the framework of regionalization proposed from Flinn and Engdahl with the changes made by Lombardi and Marzocchi and investigate the seismicity behavior into these regions. We simply applied the above mentioned methodology in the seismic catalog of each region and calculate the values of the exponential q and the correlation coefficiency. The boundaries of the Flinn-Engahl (FE regions) regions were found in the U.S Geological Survey's website (http://earthquake.usgs.gov/learn/topics/flinn_engdahl.php) and the coordinates with their names (see table 1.5.1 and 1.5.2) as well as the results are included in the following tables and graphs (see table 2.3.2.1 to 2.3.2.5 and figures 2.3.2.1, 2.3.2.2)

	q_T	corcoeff
Region 1	1,081	-0,997
Region 2* (2-3-4)	1,073	-0,996
Region 5	1,048	-0,997
Region 6	1,142	-0,996
Region 7	1,117	-0,996
Region 8	1,117	-0,997
Region 9	1,271	-0,997
Region 10	1,181	-0,998
Region 11	1,135	-0,992
Region 12	1,125	-0,998
Region 13	1,162	-0,997
Region 14*(14-15)	1,087	-0,996
Region 16	1,126	-0,999
Region 17*(17-18)	1,138	-0,997
Region 19*(19-20-21)	1,112	-0,997
Region 22*(22-23)	1,166	-0,996
Region 24	1,172	-0,998
Region 25*(25-26-27-28-47)	1,157	-0,998
Region 29	1,001	-0,999
Region 30	1,226	-0,998
Region 31	1,043	-0,992
Region 32	1,091	-0,999
Region 33	1,216	-0,997
Region 34	-	-
Region 35	-	-
Region 36	-	-
Region 37	1,353	-0,995
Region 38	-	-
Region 39	1,342	-0,986
Region 40	1,001	-0,995
Region 41	1,243	-0,982
Region 42	1,148	-0,997
Region 43	1,210	-0,997
Region 44	1,237	-0,999
Region 45	1,249	-0,998
Region 46	1,328	-0,978
Region 48	1,163	-0,995
Region 49	-	-
Region 50	-	-

Table 2.4.2.1: The q_T parameter inside the F-E regions for earthquakes with magnitude Mw≥5.0 and depth 0-150km

The symbol "-" indicates that there was not a sufficient number of earthquakes in this region in order to take a reliable result.

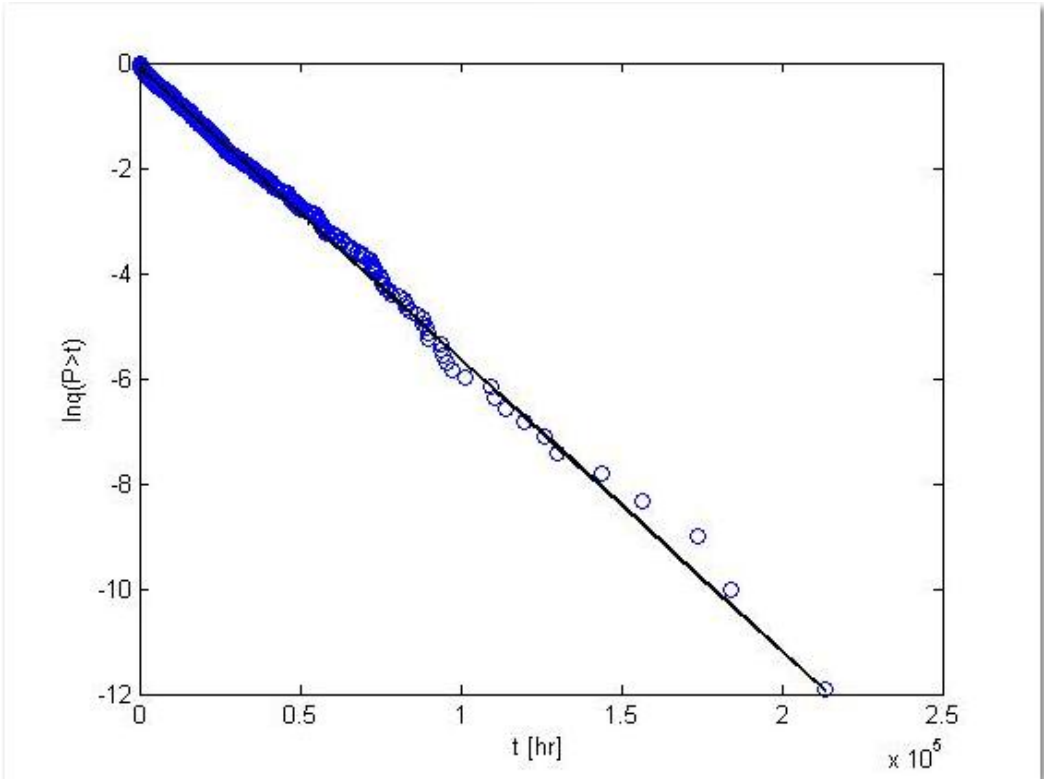

Figure 2.4.2.1: The semi-q-plot of the cumulative distribution for the interevent times for region 25 for a data set of earthquakes with magnitude equal or greater than the threshold magnitude Mw=5.0 and depth H≤150 km. The straight line represents the q-logarithmic function with value q_T=1.157.

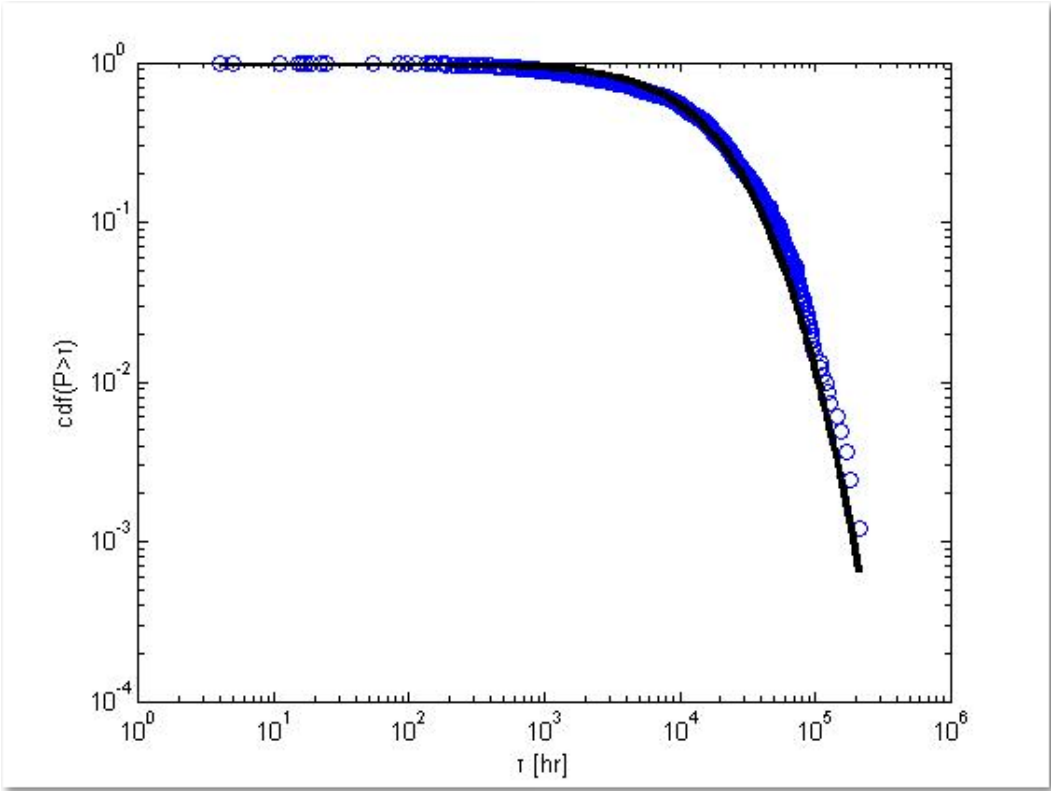

Figure 2.4.2.2:The cumulative distribution for the interevent times for region 25 for a data set of earthquakes with magnitude equal or greater than the threshold magnitude Mw=5.0 and depth H≤150 km. The value of the logarithmic function q_T is 1.063.

At this point it is becoming evidential that when we are focusing in a specific area there is a much stronger dependence between the seismic events and, according to the main principle of NESP, the investigated system is s subadditive one, that obeys at the laws of the NESP framework.

Since the above hypothesis of the NESP applied for the interevent times inside the FE regions is confirmed the following questions are born. " What happens if we discard the smaller events from the catalogs and keep only earthquakes with greater magnitude? How does the magnitude affect the system? Does the depth of the earthquakes affect our results? "

In order to answer the above questions we created three new catalogs, the first consisting of earthquakes with magnitude equal or greater than 5.5 (Mw), the second with events with magnitude equal or greater than 6.0 (Mw) for each region and a third one, in which the foreshocks and aftershocks have been removed. We applied the non-extensive statistical physics formulation, fitting the inter-event times of these events with the appropriate q-exponential function, leading to the q_T values indicated in table 2.4.2.6 and 2.4.2.7.

	q	**Corcoeff**
Region 1	1,04	-0,997
Region 2* (2-3-4)	1,001	-0,996
Region 5	1,092	-0,993
Region 6	1,113	-0,998
Region 7	1,001	-0,996
Region 8	1,086	-0,997
Region 9	1,174	-0,99
Region 10	1,05	-0,998
Region 11	1,216	-0,995
Region 12	1,071	-0,998
Region 13	1,001	-0,992
Region 14*(14-15)	1,117	-0,997
Region 16	1,065	-0,998
Region 17*(17-18)	1,343	-0,993
Region 19*(19-20-21)	1,079	-0,996
Region 22*(22-23)	1,06	-0,997
Region 24	1,124	-0,998
Region 25*(25-26-27-28-47)	1,037	-0,996
Region 29	1,09	-0,992
Region 30	1,14	-0,995
Region 31	1,001	-0,99
Region 32	1,1	-0,993
Region 33	1,069	-0,998
Region 34	-	-
Region 35	-	-

Region 36	-	-
Region 37	1,324	-0,992
Region 38	-	-
Region 39	1,265	-0,993
Region 40	1,314	-0,995
Region 41	-	-
Region 42	-	-
Region 43	1,02	-0,997
Region 44	1,075	-0,996
Region 45	1,235	-0,992
Region 46	-	-
Region 48	-	-
Region 49	-	-
Region 50	-	-

Table 2.4.2.6: The q_T parameter inside the F-E regions for a data set with earthquakes with magnitude Mw≥5.5 and depth H≤150km.

	q	**Corcoeff**
Region 1	1.02	-0,996
Region 2* (2-3-4)	1,001	-0,996
Region 5	1,001	-0,995
Region 6	1,001	-0,997
Region 7	1,161	-0,992
Region 8	1,178	-0,996
Region 9	-	-
Region 10	1,156	-0,990
Region 11	1,165	-0,991
Region 12	1,064	-0,996
Region 13	1,184	-0,959
Region 14*(14-15)	1,181	-0,998
Region 16	1,012	-0,996
Region 17*(17-18)	1,409	-0,996
Region 19*(19-20-21)	1,030	-0,996
Region 22*(22-23)	1,062	-0,997
Region 24	1,001	-0,994
Region 25*(25-26-27-28-47)	1,016	-0,996
Region 29	1,001	-0,981
Region 30	1,001	-0,994
Region 31	-	-
Region 32	1,096	-0,989
Region 33	1,011	-0,992
Region 34	-	-
Region 35	-	-
Region 36	-	-

Region 37	-	-
Region 38	-	-
Region 39	-	-
Region 40	-	-
Region 41	-	-
Region 42	-	-
Region 43	1,001	-0,993
Region 44	-	-
Region 45	1,053	-0,991
Region 46	1,449	-0,984
Region 48	-	-
Region 49	-	-
Region 50	-	-

Table 2.4.2.7: The q_T parameter inside the F-E regions for a data set with earthquakes with magnitude Mw≥6.0 and depth H≤150 km.

In order to examine how the above function is affected from the depth of the earthquakes, we created a catalog with events with seismic depth from 0 to 50 kilometers. After fitting the exponential q- function we take the results presented in Table 2.4.2.8:

	q	corcoeff
Region 1	1,070	-0,995
Region 2* (2-3-4)	1,002	-0,996
Region 5	1,037	-0,996
Region 6	1,141	-0,996
Region 7	1,154	-0,995
Region 8	1,174	-0,997
Region 9	1,133	-0,998
Region 10	1,157	-0,989
Region 11	-	-
Region 12	1,162	-0,997
Region 13	1,156	-0,995
Region 14*(14-15)	1,168	-0,998
Region 16	1,001	-0,992
Region 17*(17-18)	1,027	-0,989
Region 19*(19-20-21)	1,034	-0,990
Region 22*(22-23)	1,116	-0,993
Region 24	1,098	-0,994
Region 25*(25-26-27-28-47)	1,217	-0,997
Region 29	1,001	-0,997
Region 30	1,125	-0,997
Region 31	1,051	-0,995

Region 32	1,094	-0,999
Region 33	1,217	-0,997
Region 34	-	-
Region 35	-	-
Region 36	-	-
Region 37	1,178	-0,993
Region 38	-	-
Region 39	-	-
Region 40	1,001	-0,995
Region 41	-	-
Region 42	-	-
Region 43	1,210	-0,997
Region 44	1,237	-0,998
Region 45	1,249	-0,998
Region 46	-	-
Region 48	1,001	-0,996
Region 49	-	-
Region 50	-	-

Table 2.4.2.8: The q_T parameter inside the F-E regions for a data set with earthquakes with magnitude Mw≥5.0 and depth H≤50km.

Our last step was to examine the behavior of the " declustered catalog" , the earthquake catalog where the foreshocks and aftershocks have been removed in each F-E region. This procedure was achieved using the Reasenberg declustering method, as described in chapter 1. Then, we applied the same method of fitting the q-exponential function in the new catalog that contains only the mainshocks of the investigated period and our results are shown in table 2.4.2.9.

	q	corcoeff
Region 1	1,066	-0,998
Region 2* (2-3-4)	1,048	-0,9973
Region 5	1,038	-0,997
Region 6	1,137	-0,996
Region 7	1,11	-0,996
Region 8	1,108	-0,998
Region 9	1,269	-0,998
Region 10	1,176	-0,998
Region 11	-	-
Region 12	1,116	-0,998
Region 13	1,149	-0,997
Region 14*(14-15)	1,118	-0,999
Region 16	1,118	-0,999
Region 17*(17-18)	1,123	-0,998
Region 19*(19-20-21)	1,041	-0,997

Region 22*(22-23)	1,135	-0,998
Region 24	1,164	-0,998
Region 25*(25-26-27-28-47)	1,151	-0,999
Region 29	1,001	-0,999
Region 30	1,223	-0,997
Region 31	1,001	-0,989
Region 32	1,082	-0,999
Region 33	-	-
Region 34	-	-
Region 35	-	-
Region 36	-	-
Region 37	1,33	-0,996
Region 38	-	-
Region 39	-	-
Region 40	1,099	-0,993
Region 41	1,25	-0,98
Region 42	1,384	-0,988
Region 43	1,203	-0,998
Region 44	1,232	-0,998
Region 45	1,248	-0,998
Region 46	1,345	-0,983
Region 48	1,163	-0,995
Region 49	-	-
Region 50	-	-

Table 2.4.2.9: The q_T parameter inside the F-E regions for the declusttered data set of earthquakes with magnitude Mw≥5.0 and depth H≤150km.

Chapter 3: Conclusions

Looking back into all these procedures that have been followed in this research it is becoming obvious that the NESP model combined with geotectonic regionalization techniques can give us important information about the spatial distribution of seismic activity of the regions and the sequences of the earthquakes inside them. Furthermore, it seems that the known Poisson distribution could approximate the worldwide seismicity catalog, but when we focus on regions that are categorized according to their geological characteristics the Poisson model is no longer in position to describe the seismic behavior within each region. This seems quite rational since we are confronting a very complex system that is geologically inhomogeneous. There are regions in the earth with scarce seismic activity or no activity at all, such as Australia (Region 38), Antarctica (Region 49), Northern Eurasia (Region 50) and on the other hand extremely active regions that have given in the past very large earthquakes, mega earthquakes, such as the Sumatra earthquake with magnitude Mw=9.0 (26/12/2004) and the Japan earthquake with magnitude Mw=9,1 (11/3/2011). These are obviously regions that differ significantly on their geological properties and their faults release energy in a different way. The above are important factors that need to be taken into account in order to investigate the properties of the seismic activity and this became evidential also from the results of our research.

The calculation of the b-value from the G-R law for the worldwide catalog gave us a value that is close to 1 and as we increase the magnitude threshold from 5 to 5.5 and then to 6, the b-value becomes greater, defying the so-called high magnitude b (b_H). Looking into the G-R relation $logN(M) = a - bM$ we understand that this change is quite logical, since when we are increasing the magnitude limit we automatically decrease the total number of the earthquakes that we investigate and that leads to a higher b-value. The average of the b- value, calculated inside the seismic regions, defined by Lombardi and Marzocchi is 1.087, which is a value that differs insignificantly from the worldwide b value. The b-values estimated from eq. 2.4 are significantly greater than the values calculated from the GR law and the diagram between the estimated and the calculated values leads to a linear distribution, with all the values lying around the line as shown in figure 2.3.1.

Applying he Sotolongo-Costa and Posadas model for earthquake generation for the whole catalog we calculate an entropic index with an average of q_M=1.454 and the same result from the regionalized catalog gives us an average value for the entropic index q_M equal to 1.419. The important fact here is that we realize that the maximum values for the q_M can be found in regions that have given at least one large earthquake (Region 11, q_M=1.555, contains an earthquake of Mw=8.1, Region 8, q_M=1.516, contains earthquake of Mw=8.8, Region 19, q_M=1.507, contains earthquake with Mw=9.1). For increasing q, the physical state goes away from equilibrium, and in case of seismicity, this means that the fault planes

and fragment filling the gap between them are not in equilibrium leading to an increasing seismic activity. On the other hand, the smallest values of the parameter q_M are observed in regions, characterized by the occurrence of moderate magnitude events. When a strong earthquake occurs, more correlated behavior of the system constituents is assumed to take place, with the emergence of short and long range correlations, which induce an increase of the nonextensivity parameter q_M (Telesca, 2011).

The NESP approach to the interevent times distribution of the worldwide seismic events leads to a non-extensive thermodynamic parameter q_T that waves around 1, with an average of q_T=1.037 for the catalog that contains earthquakes with minimum magnitude Mw=5. The value q_T=1.063 estimated for the catalog with Mw(min)=5.5 ,while q_T=1.034 for the earthquake catalog with Mw(min)=6.The value q_T=1.007 estimated for the catalog that consists of earthquakes with seismic depth until 50km in agreement with the Poisson's model .

The same model, based on non extensive statistical physics, applied inside the regions estimates an average value of q_T=1.160 for events with minimum magnitude Mw=5, q_T==1.118 for Mw(min)=5.5 , q_T=1.090 for Mw(min)=6 and q_T=1.115 for earthquakes with maximum seismic depth 50km, indicating that there is a temporal connection between the earthquakes occurred inside these regions. The fact that the parameter q_T differs from 1, leads us to the conclusion that, a simple model, such as the Poisson model, is no longer the appropriate formula to describe the generation and the sequence of the earthquakes inside the FE regions and that there is an obvious need to take into consideration the complexity of the system using for our analysis a much more qualified method, such us the NESP approach.

The model used fits rather well to the observed distributions, implying the complexity of the spatiotemporal properties of seismicity and the usefulness of NESP in investigating such phenomena, exhibiting scale-free nature and long-range memory effects. Furthermore, we notice that the parameter q_T tends to decrease as we increase the magnitude threshold leading to the assumption that the correlation between them weakens when we cut out the smaller earthquakes and the conclusion that these small and moderate events take place in the generating process of the earthquakes. As far as the seismic depth is concerned we observe a negligible variation, however we cannot reach a conclusion since most of the earthquakes occurred in seismic depth until 50 km.

Chapter 4: References

Vallianatos F., G. Michas, G. Papadakis and P. Sammonds,(2012), A Non-Extensive Statistical Physics View to the Spatiotemporal Properties of the June 1995, Aigion Earthquake (M6.2) Aftershock Sequence (West Corinth Rift, Greece), Acta Geophysica vol. 60, no. 3, Jun. 2012, pp. 758-768 DOI: 10.2478/s11600-012-0011-2

Lombardi, A. M., and W. Marzocchi (2007), Evidence of clustering and nonstationarity in the time distribution of large worldwide earthquakes, J. Geophys. Res., 112, B02303, doi:10.1029/2006JB004568.

Telesca L.,(2011), Tsallis-Based Nonextensive Analysis of the Southern California Seismicity, Entropy 2011, 13, 1267-1280; doi:10.3390/e13071267

Brouers F., O. Sotolongo-Costa, K. Weron, Burr,Levy,Tsallis, (2004) , Physica A, doi:10.1016/j.physa.2004.06.008

Papadakis G., F. Vallianatos, P. Sammonds, Evidence of No Extensive Statistical Physics behavior of the Hellenic Subduction Zone seismicity ,Tectonopfysics, http://dx.doi.org/10.1016/j.tecto.2013.07.009

Telesca L., (2012) , Maximum Likelihood Estimation of the Nonextensive Parameters of the Earthquake Cumulative Magnitude Distribution, Bulletin of the Seismological Society of America, Vol. 102, No. 2, pp. 886–891, April 2012, doi: 10.1785/0120110093

Abe, S., and N. Suzuki, Law for the distance between successive earthquakes, J. Geophys. Res., 108(B2), 2113, doi:10.1029/2002JB002220, 2003.

Telesca L., Nonextensive analysis of seismic sequences, (2010) , Physica A, http://dx.doi.org/10.1016/j.physa.2010.01.012

Tsallis S., Nonadditive Entropy Sq and Nonextensive Statistical Mechanics: Applications in Geophysics and Elsewhere, (2012) , Acta Geophysica vol. 60, no. 3, Jun. 2012, pp. 502-525 DOI: 10.2478/s11600-012-0005-0

Young J.B, M.W. Presgrave, H. Aichele, D.A Wiens, E.A Flinn, The Flinn-Engdahl Regionalisation Scheme: The 1995 revision, (1996), Physics of the Earth and Planetary Interiors, Volume 96, Issue 4, September 1996, Pages 223–297, DOI: 10.1016/0031-9201(96)03141-X

Michas G.,F. Vallianatos and P. Sammonds, Non-extensivity and long-range correlations in the earthquake activity at the West Corinth rift (Greece), (2013), Nonlin. Processes Geophys., 20, 713–724, 2013, www.nonlin-processes-geophys.net/20/713/2013/doi:10.5194/npg-20-713-2013

Vallianatos F., P. Sammonds, Is plate tectonics a case of non-extensive thermodynamics?, (2010), Physica A:Statistical Mechanics and its Applications**,** Volume 389, Issue 21, 1 November 2010, Pages 4989–4993, DOI: 10.1016/j.physa.2010.06.056

Tsallis C., Introduction to Non Extensive Statistical Mechanics, (2009), ISBN 978-0-387-85358-1/ e-ISBN 978-0-387-85359-8, DOI 10.1007/978-0-387-85359-8

Tsallis, C. (1988). "Possible generalization of Boltzmann-Gibbs statistics". *Journal of Statistical Physics* **52**: 479–487. Bibcode:1988JSP....52..479T. doi:10.1007/BF01016429

Gutenberg, R., and C.F. Richter, (1944). Frequency of earthquakes in California, Bulletin of the Seismological Society of America, 34, 185-188

Flinn E. A., Engdahl E. R., 1965. A proposed basis for geographical and seismic regionalization, Rev. Geophys.,3,123–149.

Flinn E. A., Engdahl E. R., Hill A. R., 1974. Seismic and geographical regionalization, Bull, seism. Soc. Am., 64, 771–993.

Kanamori, H. and Stewart, G.S. (1978). Seismological aspects of the Guatemala earthquake of February 4, 1976. Journal of Geophysical Research 83: doi: 10.1029/JB083iB07p03427. issn: 0148-0227.

Omori, F., Investigation of aftershocks, Rep. Earthq. Inv. Comm., 2,103-39, 1894

Reasenberg, P. (1985), Second-order moment of central California seismicity, 1969-82,
J. Geophys. Res.,90, 5479-5495.3,4,5,7,8,10,11,12,18

Lay, T., and T. C. Wallace (1995). *Modern Global Seismology,* Academic Press, SanDiego, 521pp.

Vallianatos F., Michas G., Papadopoulos G., " A description of seismicity based on Non Extensive Statistical Physics: A review"

Molchan, G., and O. Dmitrieva (1992), Aftershock identication: methods and new approaches,Geophys. J. Int.,109, 501-516. 6,9,11

Scale-free statistics of time interval between successive earthquakes S Abe, N Suzuki - Physica A: Statistical Mechanics and its Applications, 2005

Analysis of Italian seismicity by using a nonextensive approach, L Telesca - Tectonophysics, 2010.

Depth-dependent time-clustering behaviour in seismicity of southern California.L Telesca, V Cuomo, V Lapenna, M Macchiato - Geophysical research letters, 2001

Long-range correlations in two-dimensional spatio-temporal seismic fluctuations, L Telesca, M Lovallo, V Lapenna, M Macchiato - Physica A: Statistical Mechanics and its Applications, 2007.

Vallianatos F., G. Michas, G. Papadakis, Non-extensive and natural time analysis of seismicity before the Mw6.4, October 12, 2013 earthquake in the South West segment of the Hellenic Arc, Physica A: Statistical Mechanics and its Applications (Impact Factor: 1.72). 11/2014; 414:163–173. DOI: 10.1016/j.physa.2014.07.038.

G. Michas, P. Sammonds, F. Vallianatos, Dynamic Multifractality in Earthquake Time Series: Insights from the Corinth Rift, Greece, Pure and Applied Geophysics (Impact Factor: 1.85). 01/2014; DOI: 10.1007/s00024-014-0875-y.

F. Vallianatos, G. Michas, G. Papadakis, A. Tzanis, Evidence of non-extensivity in the seismicity observed during the 2011–2012 unrest at the Santorini volcanic complex, Greece, Natural Hazards

and Earth System Sciences (Impact Factor: 1.83). 01/2013; 13(1):177-185. DOI: 10.5194/nhess-13-177-2013.

Presentations based on the present Thesis:

- ***Worldwide seismicity in view of non-extensive statistical physics, European Geosciences Union, Austria, Vienna, 2014.***

- ***Worldwide seismicity in view of non-extensive statistical physics, International Workshop* on *Mega Earthquakes and Tsunamis in Subduction Zones: Forecasting Approaches and Implications for Hazard Assessment, Rhodes, Greece, 2014.***

This research has been co-funded by the European Union (European Social Fund) and Greek national resources under the framework of the "THALES Program: SEISMO FEAR HELLARC" project of the "Education & Lifelong Learning" Operational Programme.

European Union
European Social Fund

OPERATIONAL PROGRAMME
EDUCATION AND LIFELONG LEARNING
investing in knowledge society
MINISTRY OF EDUCATION & RELIGIOUS AFFAIRS
MANAGING AUTHORITY

NSRF 2007-2013
programme for development
EUROPEAN SOCIAL FUND

Co-financed by Greece and the European Union